energy&fuels

pubs.acs.org/EF

Article

Influence of Ionic Liquids on the Aggregation and Pre-aggregation Phenomena of Asphaltenes in Model Solvent Mixtures by Molecular Dynamics Simulations and Quantum Mechanical Calculations

Lucas G. Celia-Silva, Rafaela N. Martins, Alfredo J. Palace Carvalho, João P. Prates Ramalho, Pedro Morgado, Eduardo J.M. Filipe, and Luís F.G. Martins*

Cite This: *Energy Fuels* 2022, 36, 9048−9065

Read Online

ACCESS | Metrics & More | Article Recommendations | Supporting Information

ABSTRACT: This work presents a systematic study of asphaltene pre-aggregation phenomena in the absence and in the presence of ionic liquids (ILs) from the family of 1-alkyl-3-methylimidazolium by molecular dynamics simulations. The effects of the alkyl chain length of the cation (studying ILs with alkyl chains between C_4 and C_{10}) and of the dimension of the anion (testing chloride and bromide) on the aggregation behavior of asphaltenes have been studied. To correlate the results obtained with the direct interaction between each additive and asphaltene, the latter was investigated both by the analysis of the radial distribution functions obtained by molecular dynamics simulations and quantum mechanical calculations. The DFT method was used to calculate the relative stability of the asphaltene-ionic liquid dimers and also the energy, shape, and spatial distribution of frontier orbitals. It was found that all the ionic liquids studied present a dispersing effect on asphaltene in model solvents, except for mixtures rich in toluene where, in most cases, the opposite effect is observed. This is accompanied by the interaction intensity as measured by radial distribution functions. The effects of the alkyl side chain length of the cation and of the anion radius are subtler, but it seems that the asphaltene dispersion effect increases with the length of the cation's alkyl side chain and decreases with the radius of the anion; these effects are more clearly observed in the mixtures richer in *n*-heptane. These trends were corroborated by DFT calculations, which showed that the energetic stability of the asphaltene-additive dimer is as higher as the alkyl chain is longer and the anion is smaller. Pre-aggregation phenomena were also studied in mixtures containing CO_2, which proved to be a precipitating agent as observed experimentally. The relative performances of the IL studied were not altered by the presence of CO_2.

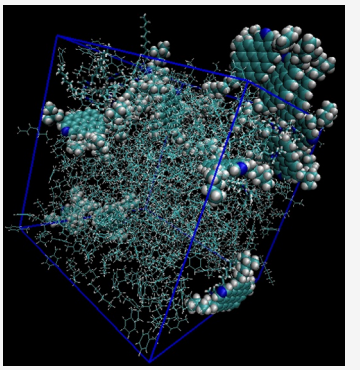

1. INTRODUCTION

One of the heaviest fractions of crude oil is asphaltenes, a general designation to a complex mixture of organic compounds, which is usually soluble in aromatic solvents, such as benzene and toluene, and insoluble in aliphatic solvents such as *n*-pentane and *n*-heptane. This behavior (which is the basis for the definition of the fraction) is a consequence of the predominant chemical nature of the substances composing the asphaltene fraction: molecules containing one or more polyaromatic cores connected to or by aliphatic chains. An asphaltene molecule composed by a single polyaromatic core (formed by 7 to 10 condensed aromatic rings) connected to aliphatic carbon chains (island or continental model) is currently the most accepted model for asphaltenes, in agreement with their experimentally determined properties.[1,2] Heteroatoms (such as N, O, and S) also play an important role in the properties of asphaltenes, as they can be present in its molecular structure both in the aromatic core and in the aliphatic chains, granting to the structure some polarity and Lewis basic character.

Because of their dimensions, chemical nature, molecular structure, geometry, and polarizability, asphaltene molecules strongly interact with each other in aliphatic hydrocarbons, forming nanoaggregates and clusters[3−5] that tend to precipitate. In oil, asphaltenes are thought to be stabilized by naturally occurring resins (substances with surfactant properties whose molecular structure resembles that of asphaltenes), clustering and forming solid deposits as a consequence of even subtle changes on operating conditions, such as temperature, pressure, and composition. These deposits may cause the clogging of pipelines and the equipment wellbores, reducing the oil flow and consequently the production rate of oil products, with high economic and environmental costs.[6]

One of the most important strategies to prevent or minimize the operative problem posed by asphaltene precipitation in the oil industry is the use of chemical additives that reduce their

Received: April 30, 2022
Revised: July 21, 2022
Published: August 3, 2022

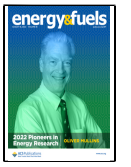

https://doi.org/10.1021/acs.energyfuels.2c01387
Energy Fuels 2022, 36, 9048−9065

aggregation tendency. The additives are, in most cases, amphiphile molecules that are able to act like natural resins, contributing to stabilize the asphaltenes in the liquid phase. Some of the most used and tested additives include alkyl phenols,[7] alkyl benzene sulfonic acids,[8−10] fatty acids, amino alcohols,[11] and polymeric substances.[12,13]

Ionic liquids (organic/inorganic salts with melting points below 100 °C) have been also considered promising candidates as asphaltene dispersing agents in oil, particularly those containing structural characteristics that allow a direct interaction with asphaltenes and/or promote compatibility with the hydrocarbon environment: one (or two) aromatic ring allowing $\pi-\pi$ stacking between asphaltenes and the additive, a long aliphatic lateral chain granting a surfactant character, acidic hydrogen atoms to interact with the asphaltene heteroatoms, and an anion with a relatively high charge density.

On the other hand, the general characteristics of ionic liquids, such as their low vapor pressure, chemical and electrochemical stability, as well as their structural diversity and tailoring ability, make them interesting choices in the present context of environmental concerns and demand of "green chemistry" characteristics.

The influence of ionic liquids on the dispersion/precipitation phenomena of asphaltenes in model solvents has been experimentally studied by a number of researchers.

Yu and Guo[14] studied the stabilizing potential of pyridinium (py^+) and isoquinolinium ($isoq^+$) based ILs with different side chain lengths and anions in CO_2-injected oil samples at high pressures. They concluded that the pyridinium and isoquinolinium based ILs with BF_4^- and PF_6^- anions presented a weaker stabilizing effect for asphaltenes than the already known alkyl benzene sulfonic acids and alkyl benzenesulfonates with a similar lateral aliphatic chain, probably due to the low charge density of the anions that hinders the additive/asphaltene charge transfer interaction. However, ILs with the same cations but with the more compact anion Cl^- (with an enhanced charge density) display a more effective stabilizing effect. This was explained by the fact that the interaction with asphaltenes can be improved by a charge density asymmetry between the IL ions. The authors concluded that the amphiphiles, as additives, are more effective the longer the alkylic chain is but not above $n = 8$, for which the effectiveness becomes almost constant. However, for the pyridinium series, the opposite trend was observed. In that work, $[C_4isoq][Cl]$ showed to be more effective in stabilizing asphaltenes than $[C_4py][Cl]$, probably because of the more extended aromatic system presented by the former. It is important to note that the presence of carbon dioxide in the system promotes asphaltene aggregation and flocculation,[15] and finding an effective stabilizing agent for those conditions is a more difficult task.

Boukherissa *et al.*[16] carried out a study of asphaltene stability using 1-propenyl-3-alkyl and 1-propylboronic acid-3-alkylimidazolium bromide as additives in toluene/*n*-heptane mixtures, concluding that ionic liquids with a boronic acid group attached to the cation are the most effective stabilizing agents due to the Lewis acid character of the boronic group. Also according to the authors, the performance of the ionic liquids increases with the length of the side chain. From the IR spectra of the ionic liquids, the authors concluded that there was a strong interaction between asphaltene and ionic liquids containing boronic groups. However, the same level of stabilization was also found for 1-butyl-3-methylimidazolium chloride but not bromide. The authors also proposed an optimal molar ratio of 1:1 between IL and asphaltenes for stabilization.

1-Butyl-3-methylimidazolium chloride was also considered the best stabilizing additive in an experimental study[17] involving also 1-butyl-3-methylimidazolium nitrate and 1-methyl-1*H*-imidazol-3-ium-2-carboxybenzoate (an amphoteric anion), with the latter being the least effective stabilizing agent. It was also found by quantum chemistry calculations that the stabilizing efficiency of these three ILs followed the LUMO−HOMO energy gap. The smaller this gap is, the higher are the reactivity of the substance and its polarizability, which enhance the interaction with asphaltenes. The interaction energy between asphaltene and 1-butyl-3-methylimidazolium chloride was found to be the highest, and the possibility of charge transfer between all the studied ILs and asphaltene was suggested.

Nezhad *et al.*[18] used 3-(2-carboxylbenzoyl)-1-methyl-1*H*-imidazol-3-ium chloride as an asphaltene dispersant in oil with a new method (involving the addition of an additive in an aqueous solution) and concluded that this IL can be used as a successful dispersing agent.

In view of the interaction with asphaltene nonpolar cores, Atta *et al.*[19] tested ILs with hydrophobic anions as stabilizing agents, namely, 1-allyl-3-methylimidazolium oleate (AMO), 1-allyl-3-methylimidazolium abietate (AMA), and 1-allyl-3-methylimidazolium cardanoxy (AMCO), directly in crude oil samples. They concluded that the dimensions of the asphaltene aggregates decrease and the dispersion efficiency increases with the increasing additive concentration, following the order AMA > AMCO > AMO. The $\pi-\pi$ stacking and charge transfer were identified as the main interaction mechanisms between additives and asphaltenes.

Ghosh *et al.*[20] tested $[C_4mim][Cl]$, $[C_4mim][Br]$, and two commercial inhibitors as additives for asphaltene dispersion in crude oil samples. Using *n*-heptane as a precipitating agent, the authors concluded that $[C_4mim][Br]$ was the most effective dispersion additive, also reducing the asphaltene onset pressure (following a depressurization procedure, the pressure at which asphaltene starts to precipitate) both in oil and in oil with carbon dioxide. The dispersive interaction between the IL cation and the aromatic rings of asphaltenes and also a steric hindrance effect associated to the bromide anion were considered the main contributors to the observed effect.

A series of imidazolium (and also pyridinium) ILs have been tested as additives to destabilize water/oil emulsions.[21] Along the $[C_nmim][Ntf_2]$ series, the destabilization potential increases with the length of the side chain. $[C_{12}mim][Ntf_2]$ was found to be the most effective. It was concluded that the additives displace the natural surface agents from the water/oil interface, leading to the destabilization of the emulsion.

Ezzat *et al.*[22] used poly(ionic liquids) with cations based on cardanol (modified using ethanolamine and tetraethylene glycol) with polysulfonate anions (QDECA and QTECA) to test their ability to disperse asphaltenes in model mixtures and to destabilize water/oil emulsions. Both additives were effective for both objectives, and it was found that the most nonpolar (QTECA) was the most efficient. The same research group had previously found a demulsifying tendency in oil/water systems for poly(ionic liquids) based on acrylate copolymers.[23]

Subramanian *et al.*[24] tested the efficiency of several ionic liquids in reducing the viscosity of heavy crude oils. The

https://doi.org/10.1021/acs.energyfuels.2c01387
Energy Fuels 2022, 36, 9048−9065

influence of the side chain length (for 3-methyl-imidazolium based IL), the anion charge density (by testing chloride, thiocyanate, and tetrafluoroborate), and the cation head group (by testing imidazolium, pyridinium, and thiazolium) was addressed. The main conclusions were as follows: (1) the longer the side chain of the cation is, the more effective is the IL to reduce viscosity, although the trend was not monotonic; (2) the reduction of viscosity increases with the anion charge density; (3) pyridinium based ILs show the highest viscosity reduction, which is more pronounced for low IL concentrations than for high concentrations. However, Santos *et al.*[25] detected an increase in the viscosity of heavy crude oils by adding 1-alkyl-3-methyl imidazolium and *N*-alkyl pyridinium based ionic liquids, which was attributed to a strong interaction between ionic liquids and the main components of crude oil that are responsible for its viscosity. The same group reported a decrease in the rigidity of the interfacial oil/water film by the addition of ionic liquids of the 1-alkyl-3-methyl imidazolium bis(trifluoromethane)sulfonamide family, which was more pronounced for the ILs with the longer side aliphatic chain.[26]

Molecular dynamics simulations and quantum mechanical methods have also been used to study the dispersion/precipitation phenomena of asphaltenes in model solvents in the presence of ionic liquids.

Hernández-Bravo *et al.*[27] studied the interaction between ionic liquids and asphaltenes by DFT calculations. They have chosen ionic liquids with a tetradecyl chain in their cation and bromide as a common anion and tested different cationic head structures (imidazolium, pyridinium, di-imidazolium, benzylimidazolium, isoquinolinium, and ammonium). They concluded that, for some ILs, the intercalation of an IL pair between two asphaltene molecules should be an energetically favorable process, in particular for isoquinolinium and benzylimidazolium based IL.

The asphaltene dispersion potential of ionic liquids was also studied by molecular dynamics simulation. In a recent work, El-Hoshoudy *et al.*[28] studied 1-hexadecyl-3-alkyl imidazolium based ILs with $FeCl_4^-$ as anion in oil samples using both experimental and simulation approaches. They concluded that these ionic liquids (with methyl, ethyl, and butyl chains connected to position 3 of the imidazolium ring) act as asphaltene dispersion agents, with the IL with the larger side alkyl chain being the more effective one. According to the authors, $\pi-\pi^*$ complexation between the ILs and the metal atoms present in asphaltenes, hydrogen bonding, and acid−base interactions between the IL anion and the asphaltene heteroatoms are the main asphaltene/IL interactions.

As previously mentioned, the presence of carbon dioxide favors the aggregation of asphaltenes. Fang *et al.*[29] studied the effect of CO_2 in a model system (composed by asphaltenes, resins, and an hydrocarbon) on the surface of silica and concluded that asphaltene precipitation is a stepwise process in which the first stage is the extraction of the nonpolar and light polar components of the asphaltene aggregates, leading to a stronger interaction between asphaltene molecules.

In this work, a systematic study of the pre-aggregation phenomena of asphaltenes in model solvents using ionic liquids as additives has been carried out using molecular dynamics simulations complemented with quantum mechanical calculations. In this first paper of a forthcoming series, the 1-alkyl-3-methyl imidazolium halide IL family has been studied. The influence of the cation alkyl side chain length and the radius of the anion on the aggregation of asphaltenes and on the asphaltene/IL interaction in toluene/*n*-heptane mixtures has been studied.

The pre-aggregation events of asphaltenes were studied by molecular dynamics simulations as a function of solvent composition in the absence and in the presence of additives from the mentioned IL family, with side chain lengths between 4 and 10 and with chloride or bromide as the anion. The dynamics of aggregation, the asphaltene/ionic liquid interaction, and the liquid structure around asphaltene have also been addressed. The energetics and the geometry of this direct interaction have been studied by DFT calculations for asphaltene/IL dimers, which provided a fundamental basis for the interpretation of the molecular dynamics simulations.

In view of their technological relevance, the influence of these ionic liquids in the aggregation of asphaltenes was also studied in systems containing carbon dioxide, which is a particularly challenging medium.

We hope that this work will contribute to a more judicious choice of the additives to be used as asphaltene precipitation inhibitors in hydrocarbon media.

2. SIMULATION DETAILS

Molecular dynamics simulations of asphaltenes in toluene/*n*-heptane mixtures with different solvent proportions have been carried out both with and without 1-alkyl-3-methylimidazolium based ionic liquids as dispersing/precipitating additives. The interaction between asphaltene and IL, as well as pre-aggregation events, has been studied from the structural and dynamic properties of the systems obtained from the analysis of simulation trajectory output files.

2.1. Models. Asphaltenes, additives, and solvent molecules were modeled within the Optimized Potentials for Liquid Simulations all-atom (OPLS-AA) force-field[30] framework, where each atom is considered as an interaction site and the potential energy is written as the sum of contributions due to bond stretching, bond angle bending, dihedral angle torsion, improper dihedral angles, and nonbonded interactions (van der Waals plus electrostatic interactions). For toluene and *n*-heptane, the parameters from the OPLS-AA original papers were used, except for the atomic partial charges of toluene, for which the reparameterization by Udier-Blagovic *et al.*[31] was employed. The validation of these parameters has been done elsewhere.[32]

A single island (continental) model molecule was chosen to describe asphaltenes. The molecular structure was designed according to the established stability rules for these compounds[33] in such a way that its main molecular properties approximately match with those experimentally obtained for one real asphaltene sample, whose experimental stability tests have been done in our laboratory. This asphaltene sample was obtained from the vacuum distillation bottom product of an oil sample from Angola. That bottom product has been kindly provided by the Portuguese oil company *Galp Energia*. This kind of distillation product was chosen because it was the one for which the asphaltene fraction is the highest and the extraction process is easier because of the absence of volatile compounds. We believe that the model used deduced from the asphaltene fraction recovered is representative of the upstream oil from these source and location.

The comparison between the properties of our model and those obtained for the real sample is shown in Table 1, and the molecular structure of the asphaltene used (along with the designation code of the most relevant atoms) is represented in

https://doi.org/10.1021/acs.energyfuels.2c01387
Energy Fuels 2022, 36, 9048−9065

Table 1. Comparison of Some Key Properties between the Asphaltene Model Chosen for the Simulations and Those Experimentally Obtained for the Real Sample

	model	experimental
M_m/g mol^{-1}	669.978	
C atoms per 1 N atom	50	45
H atoms per 1 N atom	55	57
% $C_{aliphatic}$	42	43.9
% $C_{aromatic}$	58	56.1
% $H_{aliphatic}$	81.8	87.6
% $H_{aromatic}$	18.2	12.4

Figure 1, where toluene, *n*-heptane, and a generic structure of the ionic liquids used are also represented. Even though the average molecular weight has not been determined for the real asphaltene sample, the molecular weight of the chosen molecule is within the range of the usual values reported in the literature.[34] The OPLS-AA parameterization of the asphaltene molecule was obtained using the LigParGen web server automatic parameter generators.[35] This server provides not only the OPLS-AA force-field parameters but also 1.14*CM1A, and the localized bond charge corrections (LBCCs) improved 1.14*CM1A-LBCC charges. Combined with OPLS-AA, the 1.14*CM1A[31] and the 1.14*CM1A-LBCC[36] charge models proved to be some of the most effective charge models in reproducing experimental hydration free energies. The improved 1.14*CM1A-LBCC charge model was adopted in this work.

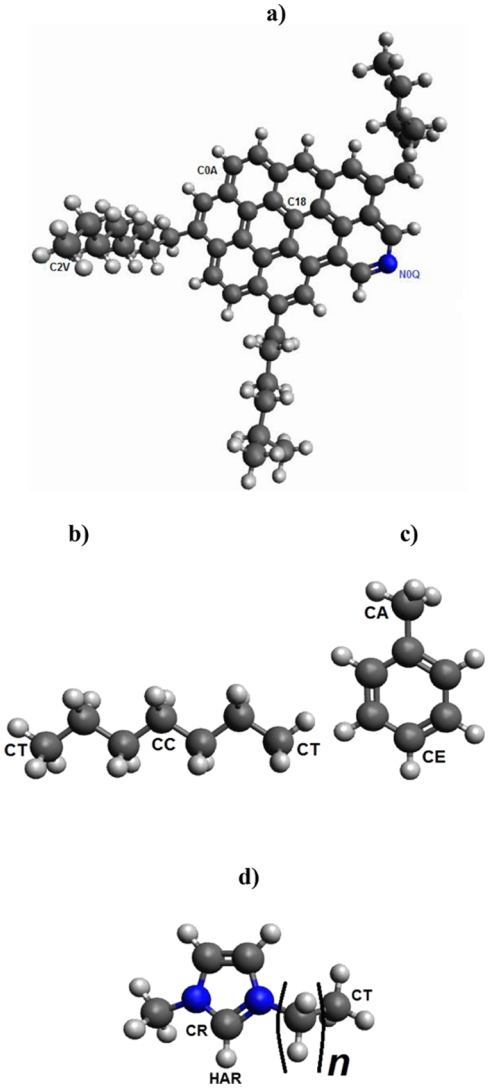

Figure 1. Molecular structure of the asphaltene model studied, the generic ionic liquid cation, and the solvents used in this work: (a) optimized 3D structure of asphaltene, (b) optimized 3D structure of *n*-heptane, (c) optimized 3D structure of toluene, and (d) optimized generic 3D structure of cations of ionic liquids. The structures include codes of relevant atoms.

The ionic liquids were modeled with the nonpolarizable version of the CL&P force field, which has been extensively used to describe this family of compounds in the last 15 years.[37,38] The original atomic partial charges were scaled by a factor of 0.8, as has been proposed for treating dynamic properties.[39]

For carbon dioxide, the EPM2 model[40] was used, which is a three-site model including partial charges, flexible angles, and rigid bonds. The nonbonded parameters for asphaltene used in the simulations are presented in the Supporting Information (Table S1 with atom codes explained in Figure S1). The parameters used for the remaining compounds can be found in the original papers of each force field, as well the functions used for all the compounds.

Following the OPLS-AA parameterization, geometrical combining rules were used to compute the nonbonded Lennard−Jones interactions between sites of different types:

$$\varepsilon_{ij} = \sqrt{\varepsilon_{ii}\varepsilon_{jj}} \quad (1)$$

$$\sigma_{ij} = \sqrt{\sigma_{ii}\sigma_{jj}} \quad (2)$$

For nonbonded interactions between sites in the same molecule, only sites separated by three or more bonds are considered. Nonbonded interactions between sites separated by three bonds are scaled by a factor of 0.5. In this work, all bonds involving hydrogen were treated as rigid, with the respective length fixed at the equilibrium distance using the LINCS algorithm.[41]

2.2. Methods. Molecular dynamics simulations were performed using GROMACS packages,[42,43] versions 5.1.5, 2016.1, and 2019.4, in cubic boxes containing 600 molecules of the solvent mixture (toluene and *n*-heptane with different proportions), 15 molecules of asphaltene, and 15 IL ion pairs (for systems where an additive is present), with periodic boundary conditions in all three directions. The initial liquid box sizes were established according to the experimental densities. For each system, the following simulation protocol was applied: an initial short simulation for system relaxation using the steepest descendent method with 1×10^6 steps followed by an NpT equilibration run of 4 ns and a 100 ns long NVT production run, which was used to obtain the structural and dynamic properties of the system. These simulations were done at 298.15 K and, for equilibration, 1 atm. For the simulations involving carbon dioxide, the production run was also done in an NpT ensemble at the same temperature and 50 atm. In this case, besides the solvent molecules, asphaltene, and additives, 300 CO_2 molecules were also added to the simulation boxes.

The equations of motion were solved using the leapfrog integration algorithm, with a time step of 1 fs, the trajectories being recorded every 1 ps during the equilibration run and every 0.5 ps for the production run. All the systems were

https://doi.org/10.1021/acs.energyfuels.2c01387
Energy Fuels 2022, 36, 9048−9065

coupled to a Nosé–Hoover thermostat[44,45] with a coupling constant of 0.2 ps and, for simulations in NpT ensembles, also coupled to a Parrinello–Rahman barostat with a coupling constant of 2 ps. An initial velocity obtained from a Maxwell distribution at the desired initial temperature has been assigned to all atoms.

Both nonbonded Lennard–Jones and electrostatic potentials were truncated by using cutoffs of 1.4 nm, and analytical tail corrections to the dispersion terms were added. The long-range electrostatic (Coulombic) interactions beyond the cutoff were calculated using the Particle Mesh Ewald (PME) sum method.[46] In the simulation protocol, the attainment of the equilibrium is confirmed by the analysis of the variations of all the energy components of the systems.

2.3. Systems. The asphaltene pre-aggregation studies by simulation were carried out in toluene/*n*-heptane solvent mixtures with and without an ionic liquid additive. Eleven molar solvent compositions for systems without additive have been used, namely, 0% (coded T0), 10% (T10), 20% (T20) 30% (T30), 40% (T40), 50% (T50), 60% (T60), 70% (T70), 80% (T80), 90% (T90), and 100% (T100) of toluene, whereas for systems with additives, five molar solvent compositions were studied (T0, T30, T50, T70, and T100). The tested additives were 1-butyl-3-methylimidazolium chloride, 1-hexyl-3-methylimidazolium chloride, 1-octyl-3-methylimidazolium chloride, 1-decyl-3-methylimidazolium chloride, and also all their bromide counterparts. The molar ratio additive/asphaltene used was 1:1. In simulations where the effect of CO_2 was tested, the same five molar solvent compositions have been used, with the molar ratio CO_2/hydrocarbon solvent being 1:2.

3. QUANTUM MECHANICAL CALCULATION DETAILS

The DFT calculations were carried out using the hybrid meta-GGA exchange correlation functional M06-2X.[47] A particular feature of this functional is that a nonlocal interaction term is included in its construction that makes it well-suited to the treatment of ionic and hydrogen bonding. Besides, the closely related functionals M06[48] and M05[49] have been successfully applied to IL. The GAMESS-US/20200930-R2[50] computational chemistry software was employed using the 6-31G(d) basis set. This basis set has been used to study asphaltene models because it yields good results for hydrogen bonding and π–π stacking interactions[51,52] while keeping a suitable computational cost.

The electronic and aggregation properties were obtained by performing a geometry optimization for all ionic pairs $[C_n\text{mim}][X]$, for different initial positions of the halide ions, and then pairing ILs and asphaltene. All calculations were performed with the convergence criteria that are used by default by the software.The optimized structures were used in vibrational frequency calculations to confirm the stationary point as minima. The absence of imaginary frequencies in all calculated vibrational spectra confirmed that the obtained structures were at their minimum energy. The interaction energy (ΔE_{int}) was obtained according to the difference of total energies between dimer and monomeric type species as shown in eq 3:

$$\Delta E_{\text{int}} = E_{ij} - (E_i + E_j) \tag{3}$$

where E_{ij} is the total energy of the interacting system, E_i is the energy of the isolated asphaltene, and E_j is the total energy of the isolated ionic pair of IL dimer.

The optimized geometries and the frontier molecular orbitals were visualized using the MacMolPlt v7.7[53] software package. The $[C_4\text{mim}][\text{Cl}]$-asphaltene system was used to screen the lowest energy structures, both in parallel and in T-shape geometries. For the remaining ionic liquids $[C_n\text{mim}][X]$ (where, n = 4, 6, 8, 10 and X = Cl, Br), dimers of IL-asphaltene were calculated in parallel geometries since they exhibited lower energies for the $[C_4\text{mim}][\text{Cl}]$ system.

From frontier orbital analysis, the energies of HOMO (E_H) and LUMO (E_L), the corresponding HOMO–LUMO gap (E_L–E_H), and also the chemical potential (μ) and hardness (η) were calculated for asphaltene and all the ionic liquids. Chemical potential and hardness were, respectively, obtained by

$$\mu = (E_L + E_H)/2 \tag{4}$$

$$\eta = (E_L - E_H)/2 \tag{5}$$

4. RESULTS AND DISCUSSION

4.1. Asphaltenes in Solvent Mixtures without Additives. The pre-aggregation dynamics, molecular interactions, and the liquid structure around asphaltene were first studied by molecular dynamics simulations in the absence of any additive.

In Figure 2, radial distribution functions [RDFs, $g(r)$] between asphaltene carbons (middle aromatic C18, Figure 1)

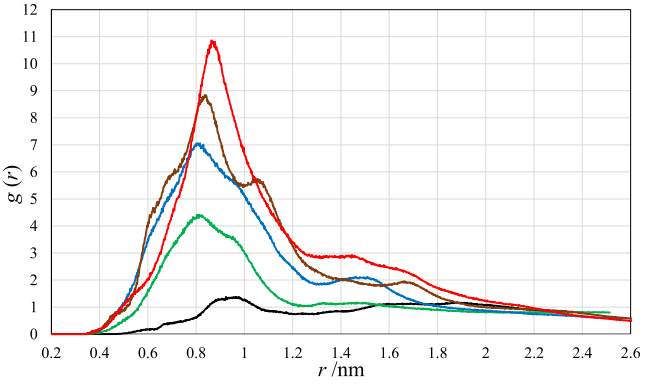

Figure 2. Radial distribution functions of the C18–C18 interaction from asphaltene molecules in toluene/*n*-heptane solvents with 100% (T100, black), 70% (T70, green), 50% (T50, blue), 30% (T30, brown), and 0% (T0, red) (molar) of toluene.

for each solvent mixture are presented. As can be seen in the figure, the interaction between aromatic carbons from different asphaltene molecules is more probable as the mole fraction of *n*-heptane increases, which is an expected result given the higher affinity of asphaltenes toward toluene and lower affinity toward *n*-heptane. A similar result was also obtained by Celia-Silva *et al.*[32] using a different asphaltene molecular model (also an island one). The radial distance corresponding to the maximum of the most intense peak changes in a non-monotonic way with the solvent composition: decreases from pure toluene (T100) to 30% in *n*-heptane (T70) and then increases with the decreasing toluene mole fraction. The transition from T100 to T70 is particularly interesting because

https://doi.org/10.1021/acs.energyfuels.2c01387
Energy Fuels 2022, 36, 9048–9065

the decrease of the distance for the maximum of the peak seems to be an indication of a structural change with the addition of *n*-heptane within this composition range. Considering that the shoulder of the T70 peak shifted to higher distances and the incipient shoulder of the T100 peak shifted to lower *r* values, it seems logical to conclude that the addition of 30% of *n*-heptane changes the relative orientation between asphaltene molecules. For T70, the closest distance between asphaltene molecules seems to be the most probable, whereas that is not observed for T100. After this structural reorganization, the most probable distance between asphaltene molecules increases as the *n*-heptane mole fraction increases.

The radial distribution functions between asphaltene (aromatic carbon C18 or the terminal alkylic carbon C2V) and toluene or *n*-heptane are represented in Figure 3 for T50

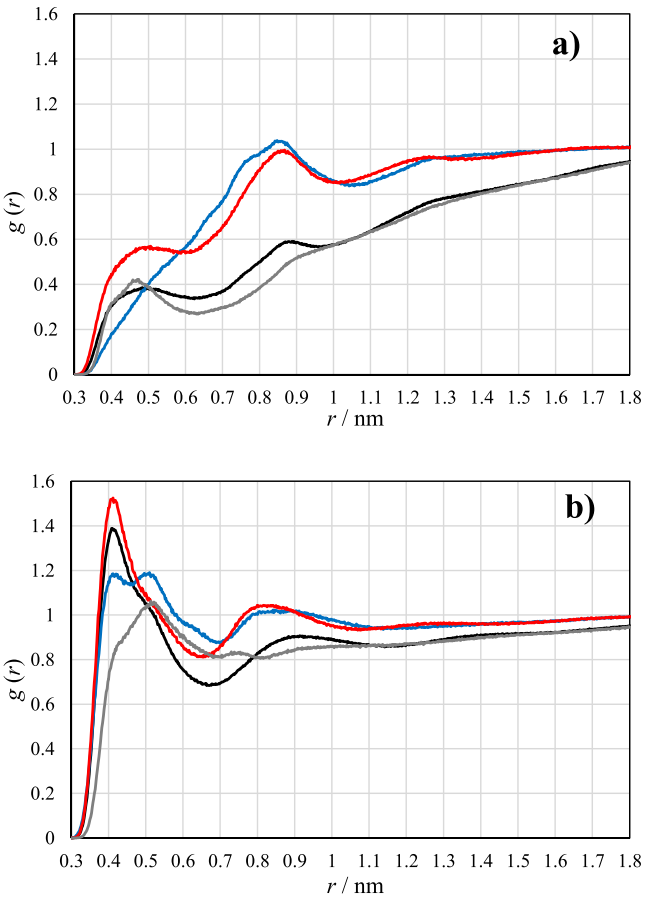

Figure 3. Radial distribution functions of toluene (*para* carbon, CE: blue and methyl carbon, CA: red) and *n*-heptane (methyl carbons, CT: black and central carbon, CC: gray) around asphaltene atoms: (a) aromatic C18 and (b) terminal aliphatic C2V.

mixtures. In the case of asphaltene C18 atom (Figure 3a), a more intense interaction with toluene (with both CA and CE atoms, Figure 1) in comparison with *n*-heptane (with both CC and CT atoms, Figure 1) can be inferred. The flexibility of alkylic groups allows them to approach closer to the C18 atom from asphaltene in the case of *n*-heptane and even for the methyl group from toluene, being however that particular orientation the least probable one. The fact that all of the RDFs in Figure 3a lie below 1 for almost the entire range reflects a difficult access to the central atom from asphaltene, which is a consequence of the strong steric hindrance that this interaction suffers, owing to the asphaltene molecular structure and the organization of its aggregates. That is not the case of the RDFs for the asphaltene−solvent interaction involving the terminal carbon of the alkyl side chains from asphaltene (C2V, Figure 1), where distinct peaks with maxima above 1 are observed, particularly for methyl groups of both solvents (Figure 3b). That is a consequence of the more exposed character of the asphaltene atom considered.

To test the organization of the solvents around asphaltene in the absence of aggregation phenomena, additional 50 (equilibration) + 20 (production) ns long simulations were carried out with just 1 asphaltene molecule and 300 molecules of each solvent. The radial distribution functions between asphaltene and each solvent for these particular simulations are represented in Figure S2 (for the same atom pairs as in Figure 3). In Figure S2a, it can be seen that the intensities of the first peaks of RDF for *n*-heptane/asphaltene (C18) interactions are very close to those of toluene (methyl carbon)/asphaltene (C18), which suggest that the existence of other asphaltene molecules excludes the approach of *n*-heptane to asphaltene C18 more effectively than the approach of toluene. In Figure S2b, the higher affinity of *n*-heptane toward the asphaltene alkyl chains in comparison with toluene is also clearer.

The asphaltene aggregation in each solvent mixture was studied, first of all, by following its dimerization phenomenon during the simulation run (100 ns). A reference atom from the asphaltene molecule is chosen (in this case, the aromatic central atom, C18), and two asphaltene molecules are considered to form a dimer whenever the distance between a pair of such atoms (each one from a different molecule) becomes lower than 8.5 Å. Since we are following a dynamic process, each molecule pair is continuously approaching and departing, and once a dimer is formed, it is only considered to disappear when the same distance exceeds 10 Å. This dual criterion is the same as that used by Goual *et al.*[7]

Using this criterion, the asphaltene dimerization events were counted, and Figure 4 represents the number of dimers (frequency, not accumulated values) as a function of its duration through a 100 ns simulation run for 11 different proportions of the two solvents.

As can be seen in the figure, the average dimer lifetime roughly decreases with the increasing percentage of toluene in the solvent. This effect is more apparent for the dimers that last the longest times. In particular, it is expected that the dimers lasting more than 2 ns should play an important role in the asphaltene aggregation process, and for these long-lasting dimers, the effect is clear despite the fact that a strict monotonic trend is not apparent because of the natural dispersion of this kind of calculations. These results show that the models used are able to capture the trend usually exhibited by the experimental determinations for asphaltenes in model solvents.

Another methodology to follow the aggregation phenomena in this kind of systems involves the calculation of the aggregation number distribution of solute molecules in the solvent. The aggregates were counted by considering the existence of an aggregate when the same chosen atom (C18 from asphaltene, in this case) for a pair of molecules is located at a distance smaller than a preselected value, in this case, 8.5 Å. Then, starting with a molecule pair, the process is repeated for a third molecule, fourth molecule, and so on. The calculations were done recurring to a program developed by Bernardes.[54] The results in the absence of any additive are

https://doi.org/10.1021/acs.energyfuels.2c01387
Energy Fuels 2022, 36, 9048−9065

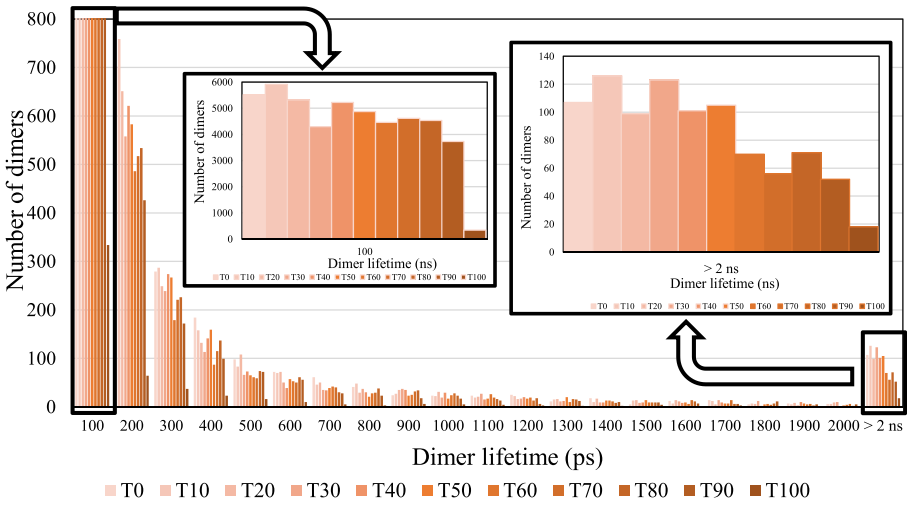

Figure 4. Histogram showing the frequency of asphaltene dimer formation as a function of its duration for 11 different solvent compositions, from 100% of toluene to 100% of *n*-heptane composition for a 100 ns production simulation (box containing 15 asphaltene molecules and 600 solvent molecules). Two insets are also shown: one for the dimers lasting up to 100 ps and the other for dimers lasting for more than 2 ns, which were amplified from each bar set of the main representation.

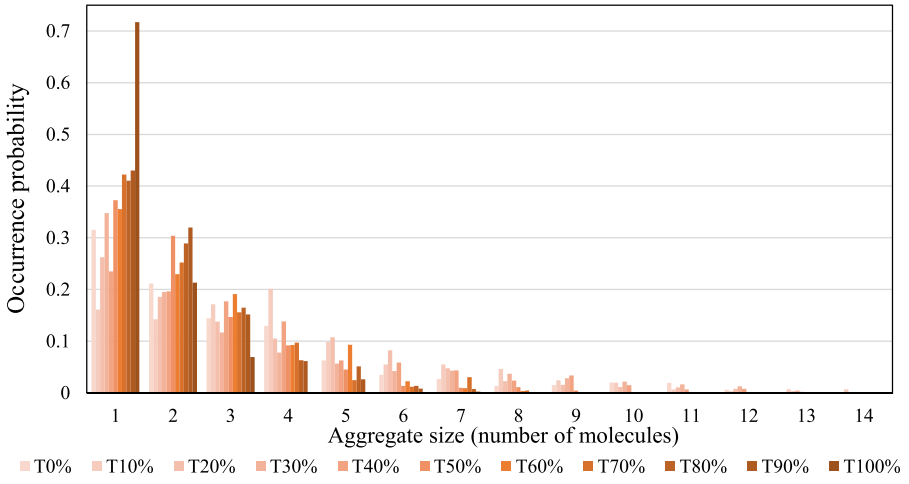

Figure 5. Occurrence probability of asphaltene aggregates as a function of aggregate dimension (number of asphaltene molecules) for 11 mixtures with different toluene/*n*-heptane proportions. The boxes contained 15 asphaltene and 600 solvent molecules.

presented in Figure 5, where the probability of the occurrence of a given aggregate (averaged over the 100 ns simulation trajectory) is represented as a function of its dimension (number of molecules). Here the value 1 means an isolated asphaltene molecule. It can be seen that as the *n*-heptane percent increases in the mixtures, the relative weight of higher dimension aggregates also increases in comparison with those of lower dimensions. Two facts are particularly revealing: the extremely high proportion of isolated asphaltene molecules in pure toluene and the absence of aggregates larger than nine for the solvent mixtures richer in toluene.

4.2. Asphaltenes and Additives in Solvent Mixtures. The influence of the presence of additives on asphaltene aggregation was studied using a simulation box containing 15 asphaltene molecules, an equal number of additive molecules, and 600 solvent molecules in five different toluene/*n*-heptane proportions during a 100 ns simulation after equilibration. The dimerization dynamics was studied in the same way as in the absence of additives, and the complete results of the dimer lifetime distribution for all the additives studied are shown in Figure S3 (Supporting Information). Given the relevance of the dimers that last more than 2 ns, the number of such dimers as a function of the solvent composition for 1-alkyl-3-methylimidazolium chloride and 1-alkyl-3-methylimidazolium bromide additives is shown in Figure 6a,b, respectively. In general, the presence of these ionic liquids tends to decrease the probability of formation of the long-lasting pairs for the mixtures that are richer in *n*-heptane (T0, T30, and T50) but seems to promote the dimer formation in pure toluene. This effect was also observed by Celia-Silva *et al.*[32] when two types of polycardanol were used as additives. On the other hand, a systematic difference between the performance of chloride and bromide based additives is not clearly observed. However, for mixtures richer in *n*-heptane, a slightly better performance (less long-lasting aggregates) of additives with the longest alkyl chains seems to be clearer for chloride based IL series.

The occurrence probability of asphaltene aggregates as a function of aggregate dimension was also obtained for asphaltenes in the absence and in the presence of all the studied additives. The results are shown in Figure 7 (chlorides) and Figure S4 (bromides), where it can be seen that, in general, all the additives act as dispersing agents for the

https://doi.org/10.1021/acs.energyfuels.2c01387
Energy Fuels 2022, 36, 9048−9065

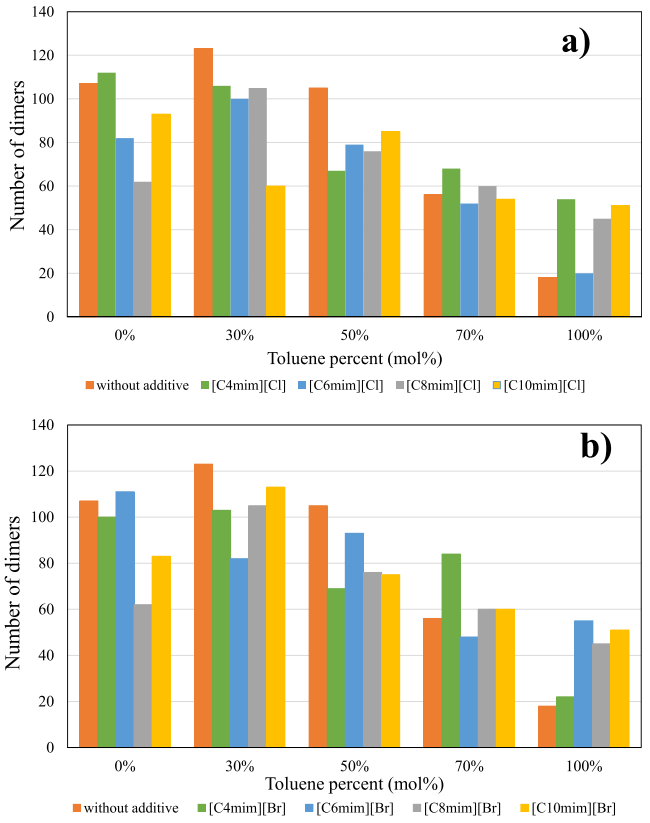

Figure 6. Histogram showing the frequency of asphaltene long-lasting (>2 ns) dimer formation as a function of toluene mole percent in the solvent mixture for systems without an additive and with each one of four different additives from the (a) 1-alkyl-3-methyl imidazolium chloride and (b) 1-alkyl-3-methyl imidazolium bromide families in a 1:1 asphaltene/additive molecular proportion.

mixtures with the highest proportions of *n*-heptane and as precipitating agents for pure toluene as solvent, with this latter effect being less pronounced for bromide additives. For systems with 70% (T70) of toluene, an intermediate behavior seems to occur with a slight tendency to the dispersion effect in particular for bromides. For instance, the addition of $[C_{10}mim][Cl]$ causes an increment of 55% of isolated asphaltenes and a reduction of 100% of asphaltene aggregates of eight molecules in comparison with the solution without additive at T0. The comparison between additives is quite difficult because of the subtle structural differences between them. Although it is almost impossible to discern a trend from the study of dimerization phenomenon, the aggregation study can give some clearer indications about the action of each additive in each environment. In general, $[C_{10}mim][Cl]$ and $[C_8mim][Br]$ seem to be the most efficient dispersing agents in mixtures containing *n*-heptane; the relative performance of the remaining additives is difficult to establish, probably being also dependent on the solvent composition. $[C_4mim][Cl]$ and $[C_4mim][Br]$ seem to be, in general, the least effective dispersing agents. For T50, the addition of $[C_{10}mim][Cl]$ causes an increment of 110% of isolated asphaltenes and a reduction of 100% of asphaltene aggregates of six molecules in comparison with the solution without additive, while for $[C_4mim][Cl]$, the increment of isolated asphaltenes is 15% and the reduction of six-molecule aggregates is 19%. This result is particularly interesting because several authors,[8,16] based on experimental determinations, have pointed out the high capacity of $[C_4mim][Cl]$ to prevent asphaltene precipitation, with an action comparable to alkylbenzene sulfonic acids. The quantitative comparison between additive performances is shown in Tables S2 and S3.

Radial distribution functions between a central atom from asphaltene (C18) in the absence and in the presence of each additive for different solvent compositions are shown in Figure 8 to evaluate the interaction intensity between asphaltene molecules for each environment. In general, the asphaltene C18−C18 interaction seems to be stronger in the absence of additives for the solvent mixtures richer in *n*-heptane, and the inverse was observed for the solvent mixtures richer in toluene, in line with the aggregate calculations. However, this interaction is, for most cases, more structured in the presence of additives, with more relative orientations available, some of them at lower distances than in the absence of additives.

Since the influence of additives on the asphaltene aggregation can be thought of as coming from some kind of specific interaction between asphaltenes and additives, the discussion about the RDFs between centers of these two components should be relevant to the problem under analysis. For this reason, RDFs between the C18 atom (and in some cases other atoms) from asphaltene and the CR, CT + CS, and anion atoms from the IL have been obtained for the eight additives studied and the five solvent compositions. CS is the generic designation of all carbon atoms from the alkyl chain of ILs except the terminal one and the two closest to the imidazolium ring. From this large amount of results, some conclusions can be drawn that are illustrated by examples of RDFs in Figure 9. Both CR (IL) and CT/CS (IL) seem to be located, on average, more closely to C18 (asphaltene) than the anion of IL, and among the CR and CT/CS, the former is usually closer to the asphaltene center than the latter. This behavior is observed for all systems, is illustrated in Figure 9a for $[C_4mim][Cl]$ as the additive for T30, and could be an indication that the asphaltene−ionic liquid interaction occurs mainly via the ionic liquid ring. In Figure 9b, RDFs between the anion and three different atoms within the asphaltene ring (C18, NOQ, and C0A) are shown for the same system at the same solvent proportion, and it is apparent that the anion is located, on average, closer to NOQ and C0A (ring edge atoms) than C18 (central atom). This general trend suggests that the anion is not in a bridging position between the asphaltene and the IL cation but preferably connected to the cation with a lateral interaction with asphaltene. This hypothesis is confirmed by the DFT calculations (Section 4.4). On the other hand, all the main peaks tend to decrease with the increasing toluene content of the solvent mixture, revealing a decreasing interaction intensity, probably because, provided that it is available, toluene competes with this specific interaction, diminishing its attraction to the ionic liquid. This is illustrated in Figure 9c for the anion peak in $[C_6mim][Br]$. In general, there is no a clear monotonic trend for the interaction intensity, measured by the peak heighs, with alkyl chain length in the two additive families, in particular for C18−CR interaction, as can be seen for instance in the systems with chlorides at T0 shown in Figure 9d. The relatively low number of molecules of each component of the interaction makes it more difficult to observe such tendencies. However, in the case of the C18−anion interaction, a slight trend of increasing the interaction intensity with the increasing of alkyl side chain length can be devised, exemplified by systems with bromide at T30 (Figure 9e). No anion effect is visible in terms of RDF

https://doi.org/10.1021/acs.energyfuels.2c01387
Energy Fuels 2022, 36, 9048−9065

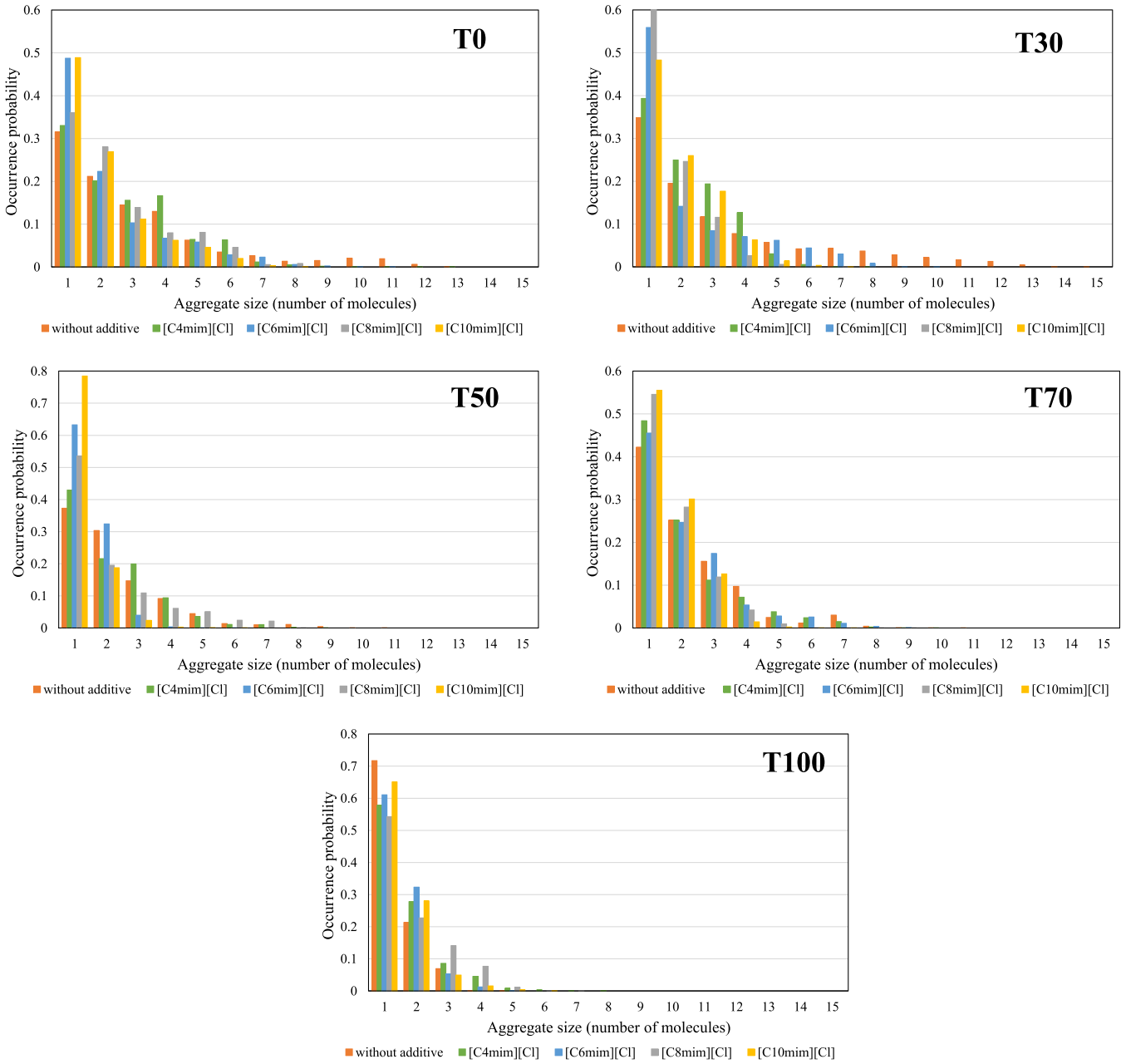

Figure 7. Occurrence probability of asphaltene aggregates as a function of aggregate dimension (number of asphaltene molecules) for systems without and with four different additives (from the 1-alkyl-3-methyl imidazolium chloride family) and five toluene/*n*-heptane proportions: 0% (T0), 30% (T30), 50% (T50), 70% (T70), and 100% (T100) toluene. All the systems present a 1:1 mole proportion between asphaltene and additive.

peak intensity, as shown in Figure 9f,g for $[C_4mim^+]$ and $[C_{10}mim^+]$, respectively, at T30. However, the peak of C18− anion appears at a distance consistently higher for bromide than for chloride, which is easily explained by the difference in the anion radius.

4.3. Asphaltenes in Solvents with Additives and Carbon Dioxide. Since carbon dioxide is a well-known precipitating agent of asphaltenes in oil, its effect on asphaltene stability in model solvents was also studied as well as the performance of the additives in toluene/*n*-heptane mixtures containing CO_2. The asphaltene aggregate distribution for such mixtures for different toluene/*n*-heptane proportions in the absence of any additive is shown in Figure S5. As can be seen, when comparing this figure with Figure 5, the presence of CO_2 seems to stimulate the formation of aggregates of higher dimensions, in particular for mixtures richer in *n*-heptane, which means that the simulations based on the models used have been able to capture the trend and behavior often observed in results obtained by experimental determinations. At T0, the addition of CO_2 causes a reduction of the smaller asphaltene aggregates up to five molecules and an increment of larger aggregates (reduction of 52% of isolated molecules and 28% of 5-molecule aggregates and an increment of 42% of 6-molecule aggregates and 13,186% of the 13-molecule aggregates) compared to the solution without CO_2. For T100, only the isolated molecules suffer a reduction (32%) by the addition of CO_2, and an increment of the other aggregate

https://doi.org/10.1021/acs.energyfuels.2c01387
Energy Fuels 2022, 36, 9048−9065

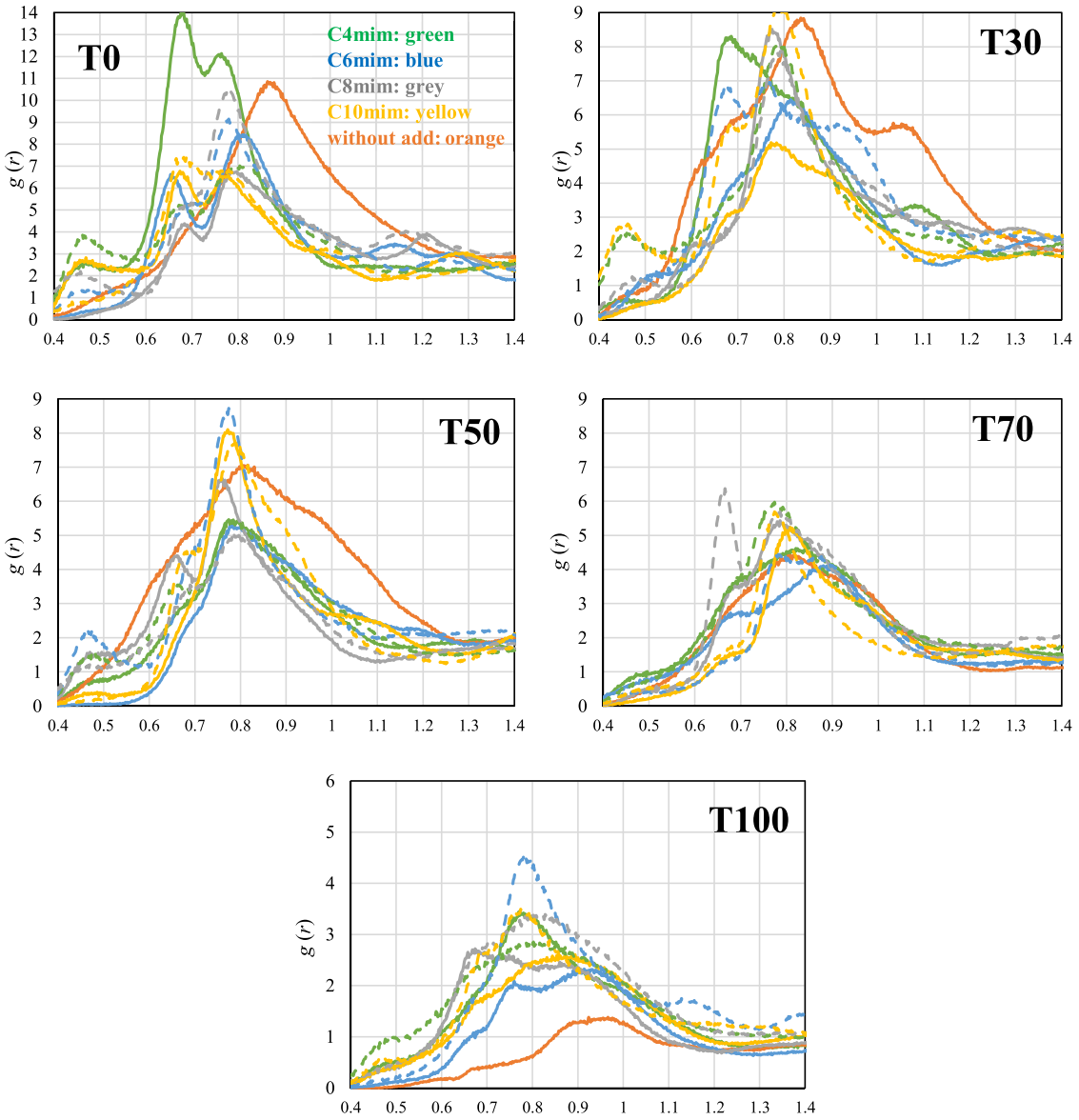

Figure 8. Radial distribution functions of C18−C18 interaction from asphaltene molecules in toluene/*n*-heptane solvent with 100% (T100), 70% (T70), 50% (T50), 30% (T30), and 0% (T0) (molar) of toluene in the absence and in the presence of 1-alkyl-3-methylimidazolium halide additives. The ionic liquids are identified by the same color code as Figures 6 and 7. Solid lines: chlorides; dashed lines: bromides (simulation snapshots in Figure S8).

dimensions is observed, reaching 40,781% for aggregates composed by four asphaltene molecules (Table S4).

In Figure 10 (chloride based IL) and Figure S6 (bromide based IL), the distribution of asphaltene aggregates is presented for the eight additives studied and for five solvent proportions in mixtures also containing CO_2. In general, the results show that, even in such solutions, the studied additives present a dispersing effect toward asphaltenes, although in a less intense fashion than in solutions without CO_2. In general, the incremented aggregates by the presence of ionic liquid are larger than in the mixtures without CO_2. For instance, for T0, six-molecule aggregates are incremented by 80% by [C_4mim][Cl] and 9% by [C_{10}mim][Cl], with the larger aggregates being reduced (Table S4). In the case of chlorides, a decrease in the dispersing performance of [C_6mim][Cl] and [C_8mim][Cl] compared with the systems without CO_2 is apparent, particularly for mixtures richer in *n*-heptane. The T70 (70% of toluene) is the solvent proportion for which the highest dispersion effect of the additives was observed, with [C_4mim][Cl] and [C_6mim][Br] being the least effective additives in this environment. On the other hand, the additive stability profile for T100 is almost equal to mixtures without CO_2, and no asphaltene dispersion effect promoted by the additives was observed. For bromide based additives, a much higher difficulty to counteract the agglomerating effect of CO_2 than the chloride counterparts was observed in T0, especially by [C_6mim][Br], with [C_{10}mim][Br] being the most efficient dispersing agent, whose performance deteriorates at T30. For mixtures with 50% of toluene or more, there is just a slight dispersion effect, with [C_{10}mim][Br] being the most effective IL. Unlike for systems without CO_2, [C_{10}mim][Br] seems to present a dispersing effect on asphaltene even in mixtures with pure toluene as solvent: the occurrence probability of all but the two smallest asphaltene aggregates is reduced by [C_{10}mim][Br], with the aggregates with five or more molecules being 100% reduced (Table S6).

https://doi.org/10.1021/acs.energyfuels.2c01387
Energy Fuels 2022, 36, 9048−9065

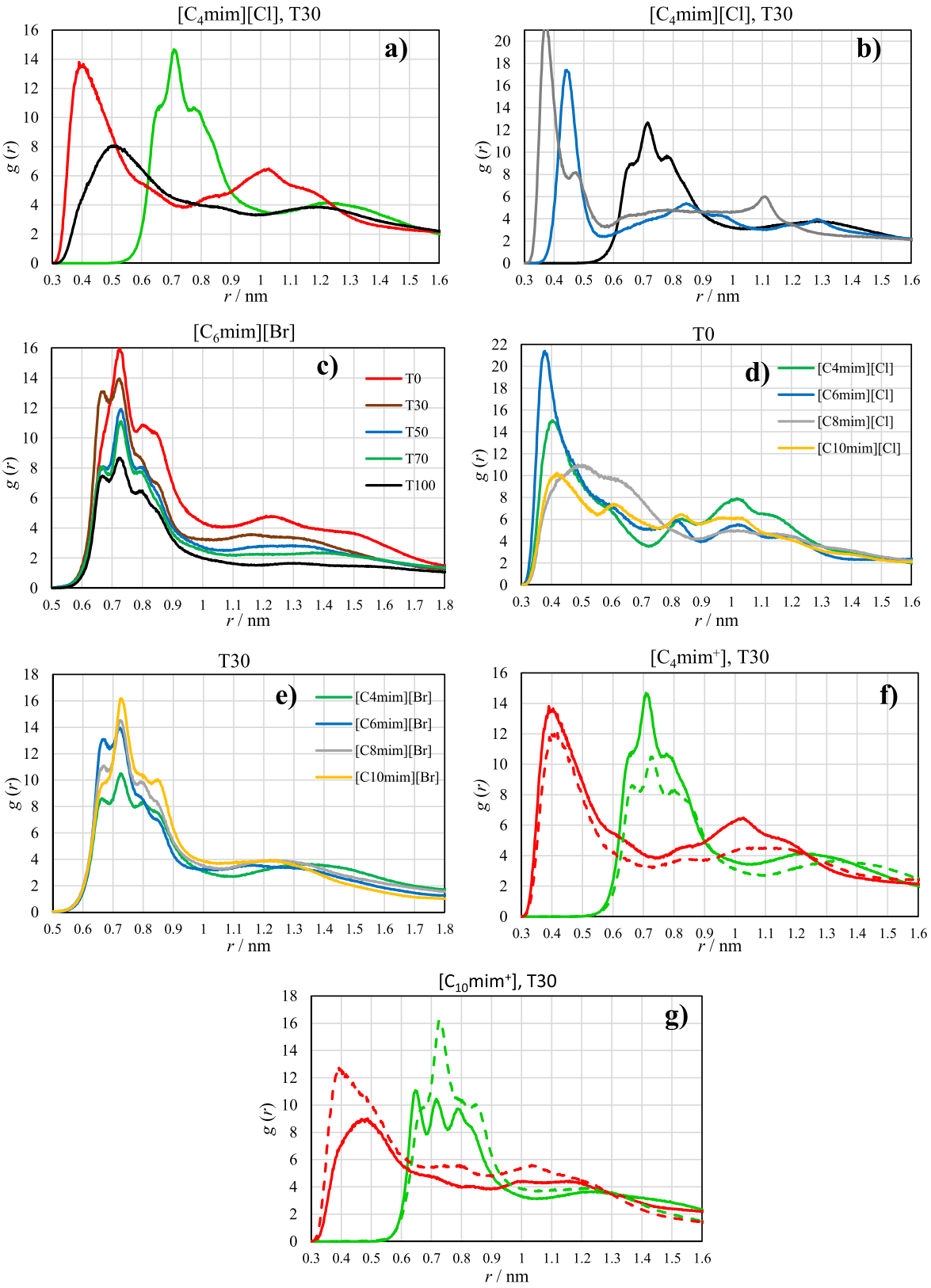

Figure 9. Radial distribution functions of the asphaltene−ionic liquid interaction: (a) black: C18−CT&CS, red: C18−CR, green: C18−anion; (b) black: C18−anion, blue: NOQ−anion, gray: C0A−anion, (c) C18−anion interaction; (d) C18−CR interaction; (e) C18−anion interaction; (f, g) the same color code as panel a; solid lines: chloride IL; dashed lines: bromide IL (simulation snapshots in Figure S8).

4.4. DFT Calculations. It has been proposed that to properly represent petroleum asphaltene structures,[55] the asphaltene monomeric model should have only one aromatic region formed by aromatic sextet carbons, with six to eight fused aromatic rings. Besides the fused aromatic rings, the asphaltene model used also possesses three aliphatic side

https://doi.org/10.1021/acs.energyfuels.2c01387
Energy Fuels 2022, 36, 9048−9065

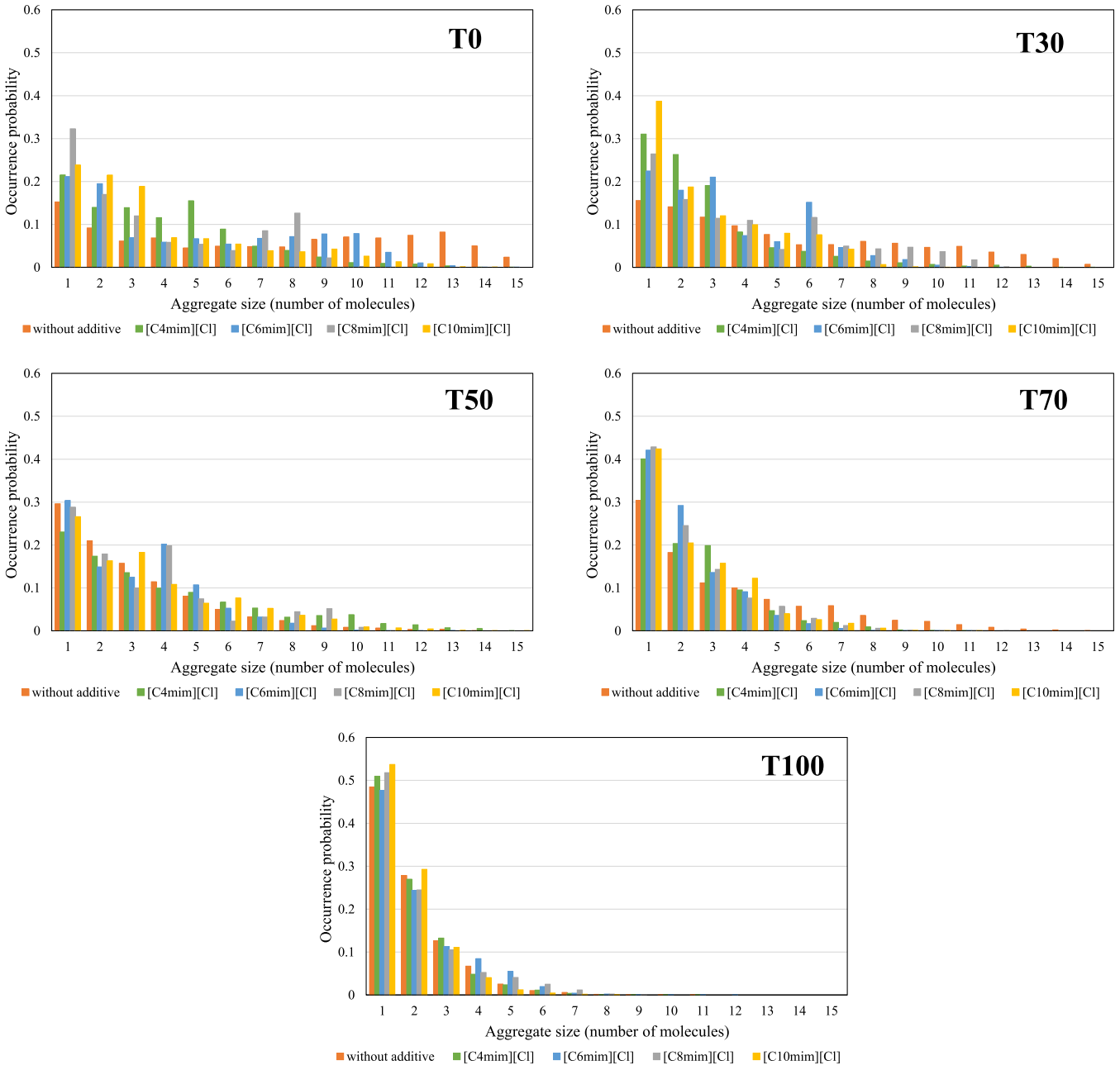

Figure 10. Occurrence probability of asphaltene aggregates as a function of aggregate dimension (number of asphaltene molecules) for systems without and with four different additives (from the 1-alkyl-3-methyl imidazolium chloride family), five toluene/*n*-heptane proportions [0% (T0), 30% (T30), 50% (T50), 70% (T70), and 100% (T100) toluene], and a fixed quantity of carbon dioxide. All the systems present a 1:1 mole proportion between asphaltene and additive and a 1:2 proportion between CO_2 and solvent.

chains and a nitrogen heteroatom. These structural characteristics define the main interactions between asphaltenes that can lead to the aggregation phenomena, notably, (*i*) the $\pi-\pi$ intermolecular interactions between asphaltene fused aromatic rings favor self-aggregation; (*ii*) aliphatic side chains can contribute to the aggregation through van der Waals attraction; and (*iii*) the heteroatom presence affects the aggregation mechanism through electrostatic interactions.[56]

Before studying the asphaltene−ionic liquid interaction, geometry optimizations were carried out on single asphaltene molecules. The optimized structure of a single asphaltene is shown in Figure S7, and as can be seen, all the aliphatic chains are disposed on the same side of the aromatic plane (side A), maximizing the long range van der Waals attraction.

The interaction between asphaltene and ionic liquids was calculated by pairing asphaltene-IL dimers to obtain the lowest energy geometries. Due to its smaller size, the [C_4mim][Cl]-asphaltene system was first optimized to obtain the lowest energy structures. Two kinds of initial structures were considered: one with the imidazolium ring of IL lying parallel to the asphaltene aromatic rings (Figure 11) and another with the imidazolium ring of the IL located perpendicular to the aromatic ring (T-shape, Figure 11). For each of the parallel and T-shape geometries, the IL was placed on the same side of asphaltene alkyl chains (side A) and on the opposite side of asphaltene alkyl chains (side B), and the anion was located both in a bridge position between the IL cation and the asphaltene and in a position further away from the asphaltene.

https://doi.org/10.1021/acs.energyfuels.2c01387
Energy Fuels 2022, 36, 9048−9065

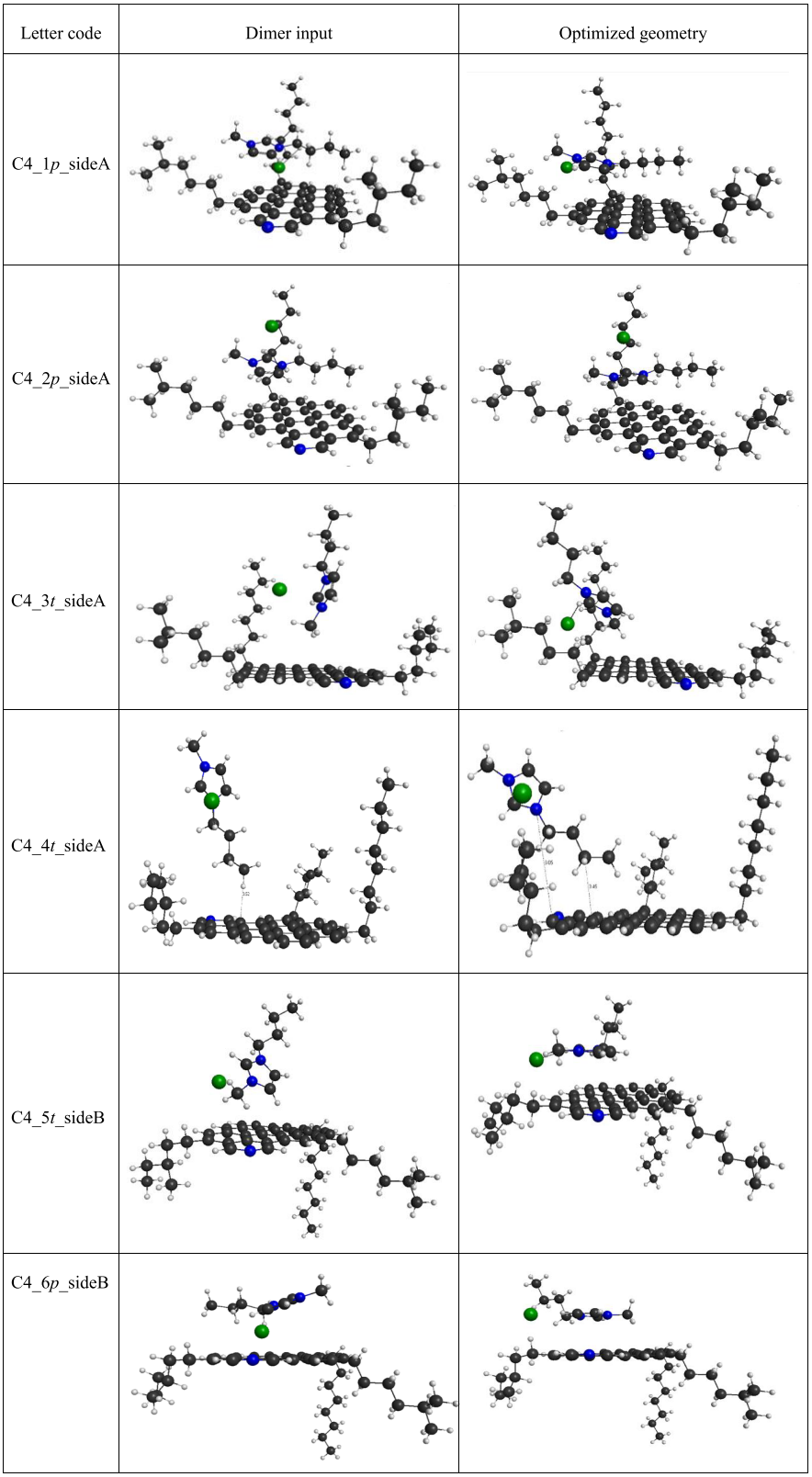

Figure 11. Input and M06-2X/6-31G(d) optimized dimer structures of [C_4mim][Cl]-asphaltene. *p* and *t* stand for parallel and T-shape structures, respectively. Side A means that IL was placed on the same side of asphaltene alkyl chains, and side B means that IL was placed on the opposite side. Notice that, in the case of side B, the initial T-shape structure has been converted into a parallel structure during the geometry optimization procedure. Atoms: carbon, dark gray; hydrogen, pale gray; nitrogen, blue; and chloride anion, green.

The chosen initial arrangements (along with a letter code) and the corresponding geometries corresponding to the lowest energies obtained are shown in Figure 11, while the energetics obtained for each position for [C_4mim][Cl]-asphaltene dimers is presented in Table 2. In this table, the total energy of each structure, the energy difference between each structure and the

https://doi.org/10.1021/acs.energyfuels.2c01387
Energy Fuels 2022, 36, 9048−9065

Table 2. Energetics of [C_4mim][Cl]-Asphaltene Dimers for M06-2X/6-31G(d) Optimized Geometries: Total Energy (E_{ij}), Difference between Each Total Energy and That of the Most Stable Structure (ΔE Geometry), and Interaction Energy (ΔE_{int})

dimer structure	$E_{ij} \times 10^{-5}$ (kJ mol^{-1})	ΔE geometry (kJ mol^{-1})	ΔE_{int} (kJ mol^{-1})
C4_5*t*_sideB	−75.5068	0.0000	−113.7154
C4_1*p*_sideA	−75.5067	3.6737	−135.0291
C4_2*p*_sideA	−75.5066	12.2680	−99.0181
C4_3*t*_sideA	−75.5065	25.9735	−87.7419
C4_6*p*_sideB	−75.5065	26.3585	−104.4906
C4_4*t*_sideA	−75.5061	65.7655	−43.0853

Table 3. Energetics of [$C_n$mim][X]-Asphaltene Dimers for M06-2X/6-31G(d) Optimized Geometries: Total Energy (E_{ij}) and Interaction Energy (ΔE_{int})

dimers	$E_{ij} \times 10^{-5}$ (kJ mol^{-1})	ΔE_{int} (kJ mol^{-1})
[C_4mim][Cl]-asphaltene	−75.5067	−135.0291
[C_6mim][Cl]-asphaltene	−77.5703	−149.1560
[C_8mim][Cl]-asphaltene	−79.6333	−166.9204
[C_{10}mim][Cl]-asphaltene	−81.6968	−160.6140
[C_4mim][Br]-asphaltene	−131.0030	−139.2243
[C_6mim][Br]-asphaltene	−133.0663	−145.1931
[C_8mim][Br]-asphaltene	−135.1294	−156.4521
[C_{10}mim][Br]-asphaltene	−137.1928	−154.4847

most stable one, and the interaction energy between asphaltene and IL for each structure are presented. The interaction energy (ΔE_{int}) was obtained using eq 3. This system was used as a starting point to optimize the other chloride and bromide based IL. The results in Table 2 are presented from the most stable dimer (C4_5t_sideB) to the less stable one (C4_4t_sideA).

Comparing the total energies of dimers, most parallel dimers exhibited lower energies than T-shape dimers. In addition, when the IL is placed on side B of asphaltene, the optimized dimers exhibited a final parallel position of imidazolium ring despite the perpendicular initial arrangement (C4_5*t*_sideB in Figure 11). It seems that the alkyl chains of asphaltene and imidazolium can interact to stabilize the dimer. The same behavior was observed by Mousavi *et al.*[57] on the role of aliphatic side chains in stabilizing the asphaltene-resin complex. This observation is also in line with the work of Takanohashi *et al.*,[58] which emphasized the stabilizing effects of aliphatic side chains in asphaltene−asphaltene interactions. In this sense, aliphatic interactions could be beneficial to stabilize ionic liquids between asphaltene molecules, avoiding asphaltene−asphaltene dimers to be formed.

The most favorable interaction energy corresponds to the structure (C4_1*p*_sideA) where the imidazolium ring lies parallel to the asphaltene rings plane and the chloride ion remains close to the rings but not between them. The T-shape dimer (C4_4*t*_sideA) revealed the lowest absolute interaction energy. In fact, optimized structures containing chloride ions bridging the aromatic and imidazolium ring plane were not observed in the optimized parallel geometries, as can be seen in Figure 11. On the contrary, the anion tends to be paired with the imidazolium ring at a significant distance from asphaltene rings.

In the case of the structures with IL on side B of the asphaltene molecule, the absence of nearby asphaltene alkyl chains to interact with the ionic pair tends to approximate the imidazolium ring toward the asphaltene fused aromatic rings, destabilizing the T-oriented configurations. Once more, the chloride ion was not found in a bridging position but lying at a distance from the asphaltene aromatic core, which is comparable to that of the imidazolium ring.

The total and interaction energies of asphaltene-[$C_n$mim]-[X] dimers, with n = 4, 6, 8, and 10 and X being Cl^- and Br^-, are shown in Table 3. Following the trends observed for [C_4mim][Cl], the dimers were arranged in such a way that the IL was placed on side A of aspahltene, with the imidazolium ring lying parallel to the aromatic core. From the values on the table, some conclusions can be drawn. First of all, the interaction energy between asphaltene and IL is strongly dependent on the alkyl chain length of the imidazolium ring, increasing (as an absolute value) as the chain length grows. The C_8mim^+ cation constitutes an exception, as it is the most interactive cation toward asphaltene, for both anions studied. However, the interaction energies presented by C_{10}mim based ILs are very close to their C_8mim counterparts, particularly for the bromide ILs. It has been suggested[10,19,59] that the capacity of the additives to prevent the asphaltene aggregation may be correlated with their ability to strongly interact with asphaltene molecules. In fact, from our simulation results discussed above, the ILs with 8 and 10 carbon atoms in the imidazolium alkyl chain are those that showed the highest capacity to prevent pre-aggregation events of asphaltene molecules for each anion studied (C_{10}mim with the chloride anion and C_8mim with the bromide anion).

On the other hand, comparing the values for the same alkyl chain length, the asphaltene−IL interaction energies are higher (as absolute values) for chloride IL than for bromide, except for C_4mim IL. This effect can be due to the highest negative charge density of chloride anion compared with bromide. However, that is a subtle difference, which is hardly reflected in their relative capacity to prevent asphaltene pre-aggregation by molecular dynamics simulations.

Atta *et al.*[19] reported that the interactions between asphaltene and imidazolium cation are responsible for reducing the viscosity of the heavy crude oils in dispersion studies. These interactions were stronger in the presence of chloride or bromide anions than the other studied anions (phenoxy anion and alkyl-substituted phenol).

In Table 4, the energies of HOMO (E_H) and LUMO (E_L), the corresponding HOMO−LUMO gap (E_L−E_H), and also the

Table 4. Chemical Potential (μ) and Hardness (η) for Asphaltene and $C_n$mim$X$ (n = 4, 6, 8, 10) (X = Cl^- and Br^-) Based on HOMO (E_H) and LUMO (E_L) Frontier Orbitals

molecular species	E_H/eV	E_L/eV	E_L−E_H/ eV	μ/eV	η/eV
asphaltene	−6.1960	−1.2871	4.9089	−3.7416	2.4545
[C_4mim][Cl]	−6.3947	0.9279	7.3226	−2.7334	3.6613
[C_6mim][Cl]	−6.3865	0.9388	7.3253	−2.7239	3.6627
[C_8mim][Cl]	−6.4355	0.9551	7.3906	−2.7402	3.6953
[C_{10}mim][Cl]	−6.3838	0.9388	7.3226	−2.7225	3.6613
[C_4mim][Br]	−6.2260	0.6395	6.8654	−2.7932	3.4327
[C_6mim][Br]	−6.2178	0.6422	6.8600	−2.7878	3.4300
[C_8mim][Br]	−6.2477	0.6748	6.9226	−2.7864	3.4613
[C_{10}mim][Br]	−6.2124	0.6449	6.8573	−2.7837	3.4286

https://doi.org/10.1021/acs.energyfuels.2c01387
Energy Fuels 2022, 36, 9048−9065

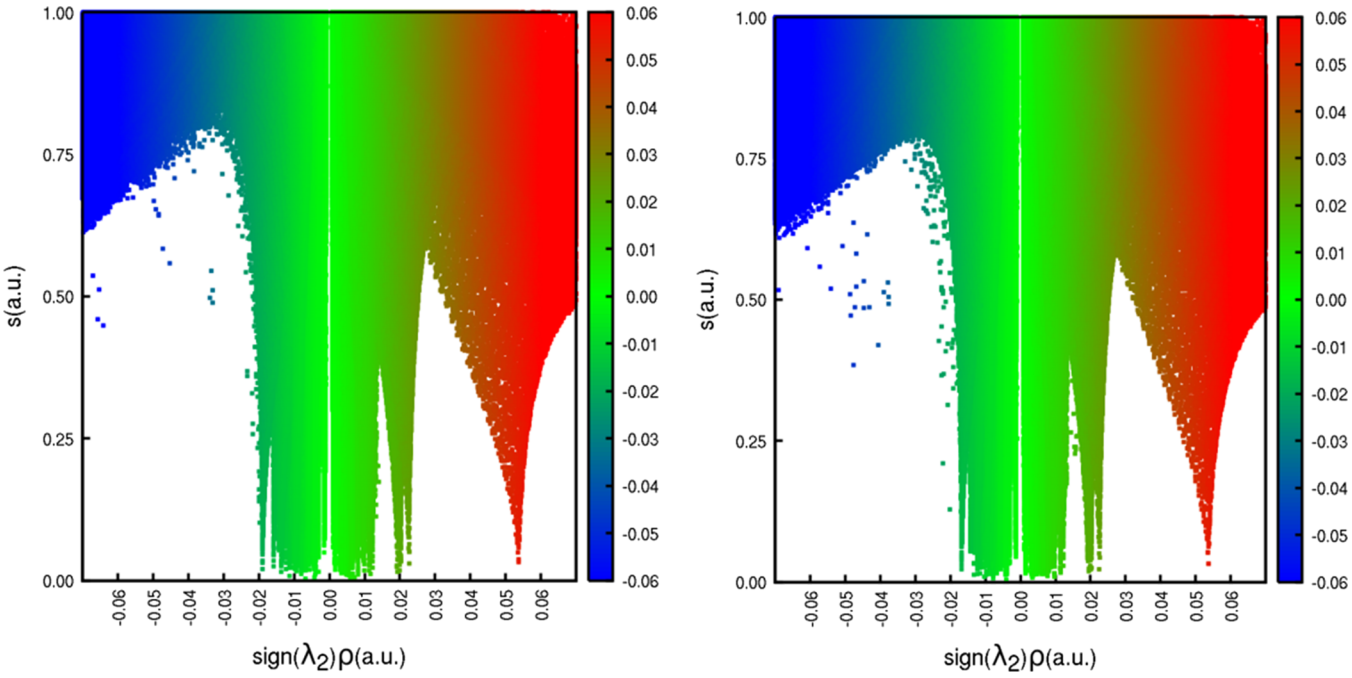

Figure 12. Reduced density gradient s versus sign(λ_2)ρ maps for the [C_8mim][Cl]-asphaltene (left) and [C_8mim][Br]-asphaltene (right) systems.

chemical potential (μ) and hardness (η) for each isolated ionic liquid and asphaltene molecule are presented.

As can be seen, the asphaltene molecule presents a lower HOMO−LUMO energy gap and a corresponding lower hardness value than any ionic liquid, which is an expected result because of its more extensive delocalized π system. For ionic liquids, the HOMO−LUMO energy gap and hardness are practically not affected by the side chain length of the cation but present lower values for bromide based ILs than for their chloride counterparts. It implies that bromide based ILs are softer molecules than chloride based ones (probably because of the bulkier character of the bromide anion), which result in a higher polarizability and reactivity potential.

In terms of chemical potential, electronic transfer between the asphaltene and ILs can be facilitated when large chemical potential differences occur between the two components. As can be seen in Table 4, all ILs present higher chemical potential values when compared to the asphaltene molecule. However, chloride compounds have slightly higher chemical potentials than bromide ones, with [C_{10}mim][Cl] and [C_6mim][Cl] presenting the highest values, which mean that the difference between the chemical potentials of asphaltene and ILs is higher for chloride based IL than for bromide ones. It is thus expected that the asphaltene-chloride IL dimers are slightly more prone to undergo charge transfer than the asphaltene-bromide IL dimers.

To gain further insights into the nature of the interactions, an AIM (atom-in-molecule) analysis was performed. The AIM (or Bader) charges were used to evaluate the charge transfer process that can occur between the asphaltene and the IL upon complexation.

Due to the weak strength of the interactions, the noncovalent interaction (NCI) method,[60] which allows a visual impression of the weak interactions, was employed. By plotting the reduced density gradient s defined as

$$s = \frac{1}{2(3\pi^2)^{1/3}} \frac{|\nabla\rho(r)|}{\rho(r)^{4/3}} \quad (6)$$

against sign(λ_2)ρ, where λ_2 is the second electron density Hessian eigenvalue, a graphical picturing of inter- and intramolecular noncovalent interactions appearing as spikes in the region of small s and sign(λ_2)ρ values is obtained. The AIM and NCI analyses were performed on the [C_8mim][Cl]-asphaltene and [C_8mim][Br]-asphaltene dimers since these systems presented the strongest interaction energies and similar geometries. The calculations were performed with the Multiwfn[61] and the NCIPLOT[60] codes.

A comparison of the Bader charges of the separated and complexed asphaltene and IL presents a small charge transfer of 0.015e in the chloride based IL case and 0.019e in bromide based IL, always from the IL to the asphaltene, which thus becomes slightly negative. This net charge transfer between the IL and asphaltene moieties is accompanied by a charge adjustment that occurs between the IL anion and cation with the anions losing electrons (0.055 and 0.061e for the Cl^- and Br^-, respectively) and the cations becoming less positive (−0.040 and −0.043e for the Cl^- and Br^- counter ions, respectively).

Figure 12 represents the 2D maps of s versus sign(λ_2)ρ for the IL-asphaltene complexes. The second density Hessian eigenvalue differentiates between the attractive or repulsive character of the interactions, being positive for attractive and negative for repulsive interactions. Colorization of the spikes according to the sign(λ_2)ρ values indicates stronger attractive interactions such as hydrogen bonds (blue), strong repulsive interaction such as steric repulsion (red), and vdW interactions (green).

As it emerges from the figure, van der Waals interactions are the main component of the interaction in both systems. Although the two graphics are quite similar, the [C_8mim][Cl]-asphaltene presents green spikes slightly shifted to the blues,

https://doi.org/10.1021/acs.energyfuels.2c01387
Energy Fuels 2022, 36, 9048−9065

reflecting a stronger interaction, which is in agreement with the calculated interaction energies.

5. CONCLUSIONS

Pre-aggregation phenomena of asphaltene molecules in model systems (*n*-heptane/toluene mixtures at varying compositions) were studied by molecular dynamics simulations in the presence and in the absence of 1-alkyl-3-methylimidazolium halides as additives with the aim of evaluating the dependence of the alkyl chain length of the cation (studying ILs with alkyl chains between C_4 and C_{10}) and the dimension of anion (testing chloride and bromide) on the aggregation behavior of asphaltenes in a systematic way. The analysis of asphaltene dimer formation as a function of its lifetime and the distribution of aggregates as a function of the number of asphaltene molecules for five different solvent compositions was done in systems with an asphaltene/additive proportion of 1:1 and also in systems containing carbon dioxide.

The results were interpreted by studying the direct interaction between each additive and asphaltene. This was done by analyzing the corresponding radial distribution functions and using DFT to calculate the relative stability, geometry, and spatial distribution of frontier orbitals of the asphaltene-ionic liquid dimers.

It was found that all the ionic liquids studied present a dispersing effect on asphaltene in model solvents, except for mixtures particularly rich in toluene, where, in most cases, they have the opposite effect. This effect correlates with the asphaltene-IL interaction intensity as measured by radial distribution functions. The influence of the alkyl side chain length and the anion radius is too subtle to be observed in a clear and unambiguous way. However, particularly in mixtures rich in *n*-heptane, increasing the alkyl side chain of the cation seems to increase the asphaltene dispersion effect, while increasing the anion radius seems to decrease it. These trends were corroborated by DFT calculations, which showed that the energetic stability of the asphaltene-additive dimer increases with the alkyl chain length of the cation, while the complex with the smaller anion is more stable. Furthermore, the AIM analysis of asphaltene-IL dimers in C_8 shows a stronger interaction for chloride based ILs than for the bromide analogues. Pre-aggregation phenomena were also studied in mixtures containing CO_2, which proved to be a precipitating agent as observed experimentally. The relative dispersing performances of the IL studied were not altered by the presence of CO_2.

Since the general objective of this kind of studies is to contribute to obtain suitable chemical additives to prevent the precipitation of asphaltenes in oil samples, this work is able to give some indications about the role played by the side alkyl chain length of the cation and the diameter of the anion of a particular family of ionic liquids in simple solvent models. Also, the dependence of the dispersing/precipitating character of the additives with the aliphatic/aromatic composition of the solvent medium has been quantitatively evaluated. These trends can be incorporated in prediction models for asphaltene precipitation as a function of the structural details of the chemical additives used and the medium properties. The influence of cation head group will be studied in future work, as well as solvent media with higher chemical complexity.

ASSOCIATED CONTENT

Supporting Information

The Supporting Information is available free of charge at https://pubs.acs.org/doi/10.1021/acs.energyfuels.2c01387.

Nonbonded parameters of asphaltene model; radial distribution functions of solvent molecules around asphaltenes; pre-aggregation results of asphaltene (dimer and aggregate formation) with bromide additives with and without carbon dioxide; optimized asphaltene monomeric model at the M06-2X/6-31G(d) level; and snapshots of the final frames of the simulations for some representative systems for RDF calculations (PDF)

AUTHOR INFORMATION

Corresponding Author

Luís F.G. Martins − *LAQV-REQUIMTE-Évora, Institute for Research and Advanced Studies, School of Science and Technology, University of Évora, Évora 7000-671, Portugal; Centro de Química Estrutural, Instituto Superior Técnico, Universidade de Lisboa, Lisboa 1049-001, Portugal;* orcid.org/0000-0001-7530-8606; Email: lfgm@uevora.pt

Authors

Lucas G. Celia-Silva − *LAQV-REQUIMTE-Évora, Institute for Research and Advanced Studies, School of Science and Technology, University of Évora, Évora 7000-671, Portugal; Centro de Química Estrutural, Instituto Superior Técnico, Universidade de Lisboa, Lisboa 1049-001, Portugal*

Rafaela N. Martins − *LAQV-REQUIMTE-Évora, Institute for Research and Advanced Studies, School of Science and Technology, University of Évora, Évora 7000-671, Portugal;* orcid.org/0000-0001-7998-6156

Alfredo J. Palace Carvalho − *LAQV-REQUIMTE-Évora, Institute for Research and Advanced Studies, School of Science and Technology, University of Évora, Évora 7000-671, Portugal*

João P. Prates Ramalho − *LAQV-REQUIMTE-Évora, Institute for Research and Advanced Studies, School of Science and Technology, University of Évora, Évora 7000-671, Portugal*

Pedro Morgado − *Centro de Química Estrutural, Instituto Superior Técnico, Universidade de Lisboa, Lisboa 1049-001, Portugal*

Eduardo J.M. Filipe − *Centro de Química Estrutural, Instituto Superior Técnico, Universidade de Lisboa, Lisboa 1049-001, Portugal*

Complete contact information is available at: https://pubs.acs.org/10.1021/acs.energyfuels.2c01387

Notes

The authors declare no competing financial interest.

ACKNOWLEDGMENTS

The team acknowledges the financial support from Fundação para a Ciência e Tecnologia by project PTDC/EQU-EQU/29458/2017 that includes European funding through FEDER (ALT-20-03-0145). L.F.G.M., R.N.M., J.P.P.R., L.G.C.S., and A.J.P.C. acknowledge the financial support from Fundação para a Ciência e Tecnologia by project CPCA/A2/4377/2020. The work was supported through project UIDB/50006/2020| UIDP/50006/2020 funded by FCT/MCTES through national

funds. Centro de Química Estrutural acknowledges the financial support from Fundação para a Ciência e Tecnologia (UIDB/00100/2020).

REFERENCES

(1) Schuler, B.; Meyer, G.; Peña, D.; Mullins, O. C.; Gross, L. Unraveling the Molecular Structures of Asphaltenes by Atomic Force Microscopy. *J. Am. Chem. Soc.* **2015**, *137*, 9870−9876.
(2) Alvarez-Ramírez, F.; Ruiz-Morales, Y. Island versus Archipelago Architecture for Asphaltenes: Polycyclic Aromatic Hydrocarbon Dimer Theoretical Studies. *Energy Fuels* **2013**, *27*, 1791−1808.
(3) Mullins, O. C. The Modified Yen Model. *Energy Fuels* **2010**, *24*, 2179−2207.
(4) Mullins, O. C.; Sabbah, H.; Eyssautier, J.; Pomerantz, A. E.; Barré, L.; Andrews, A. B.; Ruiz-Morales, Y.; Mostowfi, F.; McFarlane, R.; Goual, L.; et al. Advances in Asphaltene Science and the Yen−Mullins Model. *Energy Fuels* **2012**, *26*, 3986−4003.
(5) Goual, L.; Sedghi, M.; Mostowfi, F.; McFarlane, R.; Pomerantz, A. E.; Saraji, S.; Mullins, O. C. Cluster of Asphaltene Nanoaggregates by DC Conductivity and Centrifugation. *Energy Fuels* **2014**, *28*, 5002−5013.
(6) Mullins, O. C.; Sheu, E. Y.; Hammani, A.; Marchall, A. G., Eds., *Asphaltenes, Heavy Oils and Petroleomics*; Springer: New York, 2007.
(7) Goual, L.; Sedghi, M.; Wang, X.; Zhu, Z. Asphaltene Aggregation and Impact of Alkylphenols. *Langmuir* **2014**, *30*, 5394−5403.
(8) Chang, C. L.; Fogler, H. S. Stabilization of Asphaltenes in Aliphatic Solvents Using Alkylbenzene-Derived Amphiphiles. 1. Effect of the Chemical Structure of Amphiphiles on Asphaltene Stabilization. *Langmuir* **1994**, *10*, 1749−1757.
(9) Chang, C. L.; Fogler, H. S. Stabilization of Asphaltenes in Aliphatic Solvents Using Alkylbenzene-Derived Amphiphiles. 2. Study of the Asphaltene-Amphiphile Interactions and Structures Using Fourier Transform Infrared Spectroscopy and Small-Angle X-ray Scattering Techniques. *Langmuir* **1994**, *10*, 1758−1766.
(10) Goual, L.; Sedghi, M. Role of ion-pair interactions on asphaltene stabilization by alkylbenzenesulfonic acids. *J. Col. Int. Sci.* **2015**, *440*, 23−31.
(11) Chávez Miyauchi, T. E.; Zamudio-Rivera, L. S.; Barba-López, V.; Buenrostro-Gonzalez, E.; Martínez-Magadán, J. M. N-aryl amino-alcohols as stabilizers of asphaltenes. *Fuel* **2013**, *110*, 302−309.
(12) Kraiwattanawong, K.; Fogler, H. S.; Gharfeh, S. G.; Singh, P.; Thomason, W. H.; Chavadej, S. Effect of Asphaltene Dispersants on Aggregate Size Distribution and Growth. *Energy Fuels* **2009**, *23*, 1575−1582.
(13) Palermo, L. C. M.; Lucas, E. F. Asphaltene Aggregation: Influence of Composition of Copolymers Based on Styrene-Stearyl Methacrylate and Styrene-Stearyl Cinnamate Containing Sulfate Groups. *Energy Fuels* **2016**, *30*, 3941−3946.
(14) Hu, Y.-F.; Guo, T.-M. Effect of the Structures of Ionic Liquids and Alkylbenzene-Derived Amphiphiles on the Inhibition of Asphaltene Precipitation from CO2-Injected Reservoir Oils. *Langmuir* **2005**, *21*, 8168−8174.
(15) Soroush, S.; Straver, E. J. M.; Rudolph, E. S. J.; Peters, C. J.; de Loos, T. W.; Zitha, P. L. J.; Vafaie-Sefti, M. Phase behavior of the ternary system carbon dioxide + toluene + asphaltene. *Fuel* **2014**, *137*, 405−411.
(16) Boukherissa, M.; Mutelet, F.; Modarressi, A.; Dicko, A.; Dafri, D.; Rogalski, M. Ionic Liquids as Dispersants of Petroleum Asphaltenes. *Energy Fuels* **2009**, *23*, 2557−2564.
(17) Ogunlaja, A. S.; Hosten, E.; Tshentu, Z. R. Dispersion of Asphaltenes in Petroleum with Ionic Liquids: Evaluation of Molecular Interactions in the Binary Mixture. *Ind. Eng. Chem. Res.* **2014**, *53*, 18390−18401.
(18) Nezhad, E. R.; Heidarizadeh, F.; Sajjadifar, S.; Abbasi, Z. Dispersing of Petroleum Asphaltenes by Acidic Ionic Liquid and Determination by UV-Visible Spectroscopy. *J. Pet. Eng.* **2013**, No. 203036.
(19) Atta, A. M.; Ezzat, A. O.; Abdullah, M. M.; Hashem, A. H. Effect of Different Families of Hydrophobic Anions of Imadazolium Ionic Liquids on Asphaltene Dispersants in Heavy Crude Oil. *Energy Fuels* **2017**, *31*, 8045−8053.
(20) Ghosh, B.; Sulemana, N.; Banat, F.; Mathew, N. Ionic liquid in stabilizing asphaltenes during miscible CO2 injection in high pressure oil reservoir. *J. Pet. Sci. Eng.* **2019**, *180*, 1046−1057.
(21) Silva, E. B.; Santos, D.; Alves, D. R. M.; Barbosa, M. S.; Guimarães, R. C. L.; Ferreira, B. M. S.; Guarnieri, R. A.; Franceschi, E.; Dariva, C.; Santos, A. F.; et al. Demulsification of Heavy Crude Oil Emulsions Using Ionic Liquids. *Energy Fuels* **2013**, *27*, 6311−6315.
(22) Ezzat, A. O.; Atta, A. M.; Al-Lohedan, H. A.; Abdullah, M. M. S.; Hashem, A. I. Synthesis and Application of Poly(ionic liquid) Based on Cardanol as Demulsifier for Heavy Crude Oil Water Emulsions. *Energy Fuels* **2018**, *32*, 214−225.
(23) Abdullah, M. M. S.; Al-Lohedan, H. A.; Attah, A. M. Synthesis and application of amphiphilic ionic liquid based on acrylate copolymers as demulsifier and oil spill dispersant. *J. Mol. Liq.* **2016**, *219*, 54−62.
(24) Subramanian, D.; Wu, K.; Firoozabadi, A. Ionic liquids as viscosity modifiers for heavy and extra-heavy crude oils. *Fuel* **2015**, *143*, 519−526.
(25) Santos, R. L. M.; Filho, E. B. M.; Dourado, R. S.; Santos, A. F.; Borges, G. R.; Dariva, C.; Santana, C. C.; Franceschi, E.; Santos, D. Study on the use of aprotic ionic liquids as potential additives for crude oil upgrading, emulsion inhibition, and demulsification. *Fluid Phase Equilib.* **2019**, *489*, 8−15.
(26) Alves, D.; Lourenço, E.; Franceschi, E.; Santos, A. F.; Santana, C. C.; Borges, G.; Dariva, C. Influence of Ionic Liquids on the Viscoelastic Properties of Crude Oil Emulsions. *Energy Fuels* **2017**, *31*, 9132−9139.
(27) Hernández-Bravo, R.; Miranda, A. D.; Martínez-Magadán, J. M.; Domínguez, J. M. Experimental and Theoretical Study on Supramolecular Ionic Liquid (IL)−Asphaltene Complex Interactions and Their Effects on the Flow Properties of Heavy Crude Oils. *J. Phys. Chem. B* **2018**, *122*, 4325−4335.
(28) El-Hoshoudy, A. N.; Ghanem, A.; Desouky, S. M. Imidazolium-based ionic liquids for asphaltene dispersion; experimental and computational studies. *J. Mol. Liq.* **2021**, *324*, 114469829.
(29) Fang, T.; Wang, M.; Li, J.; Liu, B.; Shen, Y.; Yan, Y.; Zhang, J. Study on the Asphaltene Precipitation in CO_2 Flooding: A Perspective from Molecular Dynamics Simulation. *Ind. Eng. Chem. Res.* **2018**, *57*, 1071−1077.
(30) Jorgensen, W. L.; Maxwell, D. S.; Tirado-Rives, J. Development and Testing of the OPLS All-Atom Force Field on Conformational Energetics and Properties of Organic Liquids. *J. Am. Chem. Soc.* **1996**, *118*, 11225−11236.
(31) Udier−Blagovic, M.; Tirado, P. M.; Pearlman, S. A.; Jorgensen, W. L. Accuracy of free energies of hydration using CM1 and CM3 atomic charges. *J. Comput. Chem.* **2004**, *25*, 1322−1332.
(32) Celia-Silva, L. G.; Vilela, P. B.; Morgado, P.; Lucas, E. F.; Martins, L. F. G.; Filipe, E. J. M. Pre-aggregation of asphaltenes in presence of natural polymers by molecular dynamics simulation. *Energy Fuels* **2020**, *34*, 1581−1591.
(33) Law, J. C.; Headen, T. F.; Jiménez-Serratos, G.; Boek, E. S.; Murgich, J.; Müller, E. A. Catalogue of Plausible Molecular Models for the Molecular Dynamics of Asphaltenes and Resins Obtained from Quantitative Molecular Representation. *Energy Fuels* **2019**, *33*, 9779−9795.
(34) Mullins, O. C. Asphaltenes. *Annu. Rev. Anal. Chem.* **2011**, *4*, 393−418.
(35) Dodda, L. S.; Cabeza de Vaca, I.; Tirado-Rives, J.; Jorgensen, W. L. LigParGen web server: an automatic OPLS-AA parameter generator for organic ligands. *Nucl. Acids Res.* **2017**, *45*, W331−W336.
(36) Dodda, L. S.; Vilseck, J. Z.; Tirado-Rives, J.; Jorgensen, W. L. 1.14*CM1A-LBCC: Localized Bond-Charge Corrected CM1A Charges for Condensed-Phase Simulations. *J. Phys. Chem. B* **2017**, *121*, 3864−3870.

https://doi.org/10.1021/acs.energyfuels.2c01387
Energy Fuels 2022, 36, 9048−9065

(37) Canongia Lopes, J. N.; Deschamps, J.; Pádua, A. A. H. Modeling Ionic Liquids Using a Systematic All-Atom Force Field. *J. Phys. Chem. B* **2004**, *108*, 2038−2047.
(38) Canongia Lopes, J. N.; Pádua, A. A. H. CL&P: A generic and systematic force field for ionic liquids modeling. *Theor. Chem. Acc.* **2012**, *131*, 1129.
(39) Chaban, V. V.; Voroshylova, I. V.; Kalugin, O. N. A new force field model for the simulation of transport properties of imidazolium-based ionic liquids. *Phys. Chem. Chem. Phys.* **2011**, *13*, 7910−792039.
(40) Harris, J. G.; Yungt, K. H. Carbon Dioxide's Liquid-Vapor Coexistence Curve and Critical Properties as Predicted by a Simple Molecular Model. *J. Phys. Chem.* **1995**, *99*, 12021−12024.
(41) Hess, B.; Bekker, H.; Berendsen, H. J. C.; Fraaije, J. G. E. M. LINCS: A Linear Constraint Solver for Molecular Simulations. *J. Comput. Chem.* **1997**, *18*, 1463−1472.
(42) Van Der Spoel, D.; Lindahl, E.; Hess, B.; Groenhof, G.; Mark, A. E.; Berendsen, H. J. C. GROMACS: Fast, flexible and free. *J. Comput. Chem.* **2005**, *26*, 1701−1718.
(43) Pronk, S.; Páll, S.; Schulz, R.; Larsson, P.; Bjelkmar, P.; Apostolov, R.; Shirts, M. R.; Smith, J. C.; Kasson, P. M.; van der Spoel, D.; et al. GROMACS 4.5: a high-throughput and highly parallel open source molecular simulation toolkit. *Bioinformatics* **2013**, *29*, 845−854.
(44) Nosé, S. A molecular dynamics method for simulations in the canonical ensemble. *Mol. Phys.* **1984**, *52*, 255−268.
(45) Hoover, W. G. Canonical dynamics: Equilibrium phase-space distributions. *Phys. Rev. A* **1985**, *31*, 1695−1697.
(46) Toukmaji, A. Y.; Board, J. A., Jr. Ewald summation techniques in perspective: a survey. *Comput. Phys. Commun.* **1996**, *95*, 73−92.
(47) Zhao, Y.; Truhlar, D. G. The M06 suite of density functionals for main group thermochemistry, thermochemical kinetics, noncovalent interactions, excited states, and transition elements: two new functionals and systematic testing of four M06-class functionals and 12 other functionals. *Theor. Chem. Acc.* **2008**, *120*, 215−241.
(48) Mercy, M.; Rebecca Taylor, S. F.; Jacquemin, J.; Hardacre, C.; Bell, R. G.; de Leeuw, N. H. The addition of CO2 to four superbase ionic liquids: a DFT study. *Phys. Chem. Chem. Phys.* **2015**, *17*, 28674−28682.
(49) Izgorodina, E. I.; Bernard, U. L.; MacFarlane, D. R. Ion-Pair Binding Energies of Ionic Liquids: Can DFT Compete with Ab Initio-Based Methods? *J. Phys. Chem. A* **2009**, *113*, 7064−7072.
(50) Barca, G. M. J.; Bertoni, C.; Carrington, L.; Datta, D.; De Silva, N.; Deustua, J. E.; Fedorov, D. G.; Gour, J. R.; Gunina, A. O.; Guidez, E.; et al. Recent developments in the general atomic and molecular electronic structure system. *J. Chem. Phys.* **2020**, *152*, 154102.
(51) Costa, L. M.; Hayaki, S.; Stoyanov, S. R.; Gusarov, S.; Tan, X.; Gray, M. R.; Stryker, J. M.; Tykwinsk, R.; Carneiro, J. W. M.; Sato, H.; et al. 3D-RISM-KH molecular theory of solvation and density functional theory investigation of the role of water in the aggregation of model asphaltenes. *Phys. Chem. Chem. Phys.* **2012**, *14*, 3922−3934.
(52) Andrews, A. B.; Wang, D.; Marze, K. M.; Mullins, O. C.; Crozier, K. B. Surface enhanced Raman spectroscopy of polycyclic aromatic hydrocarbons and molecular asphaltenes. *Chem. Phys. Lett.* **2015**, *620*, 139−143.
(53) Bode, B. M.; Gordon, M. S. MacMolPlt: A graphical user interface for GAMESS. *J. Mol. Graphics Modell.* **1998**, *16*, 133−138.
(54) Bernardes, C. E. S. AGGREGATES: Finding structures in simulation results of solutions. *J. Comput. Chem.* **2017**, *38*, 753−765.
(55) Castellano, O.; Gimon, R.; Soscun, H. Theoretical Study of the σ-π and π-π Interactions in Heteroaromatic Monocyclic Molecular Complexes of Benzene, Pyridine, and Thiophene Dimers: Implications on the Resin-Asphaltene Stability in Crude Oil. *Energy Fuels* **2011**, *25*, 2526−2541.
(56) Ekramipooya, A.; Valadi, F. M.; Farisabadi, A.; Gholami, M. R. Effect of the heteroatom presence in different positions of the model asphaltene structure on the self-aggregation: MD and DFT study. *J. Mol. Liq.* **2021**, *334*, No. 116109.
(57) Mousavi, M.; Abdollahi, T.; Pahlavan, F.; Fini, E. H. The influence of asphaltene-resin molecular interactions on the colloidal stability of crude oil. *Fuel* **2016**, *183*, 262−271.
(58) Takanohashi, T.; Sato, S.; Saito, I.; Tanaka, R. Molecular Dynamics Simulation of the Heat-Induced Relaxation of Asphaltene Aggregates. *Energy Fuels* **2003**, *17*, 135−139.
(59) Hernández-Bravo, R.; Miranda, A. D.; Martínez-Mora, O.; Domínguez, Z.; Martínez-Magadán, J. M.; García-Chávez, R.; Domínguez-Esquival, J. M. Calculation of the Solubility Parameter by COSMO-RS Methods and Its Influence on Asphaltene−Ionic Liquid Interactions. *Ind. Eng. Chem. Res.* **2017**, *56*, 5107−5115.
(60) Johnson, E. R.; Keinan, S.; Mori-Sánchez, P.; Contreras-Garcia, J.; Cohen, A. J.; Yang, W. Revealing Noncovalent Interactions. *J. Am. Chem. Soc.* **2010**, *132*, 6498−6506.
(61) Lu, T.; Chen, F. Multiwfn: A Multifunctional Wavefunction Analyzer. *J. Comput. Chem.* **2012**, *33*, 580−592.

https://doi.org/10.1021/acs.energyfuels.2c01387
Energy Fuels 2022, 36, 9048−9065